and Glut1, respectively) [3], where it is converted into glycogen. Increasing capacity of glucose uptake in the skeletal muscle is considered beneficial for the prevention and treatment of type 2 diabetes [3,4]. On the other hand, glucose metabolism in the skeletal muscle may affect the whole body metabolism; the skeletal muscle-specific inactivation of *Glut4* has resulted in defect in insulin action in the adipose tissue (glucose uptake) and liver (suppression of gluconeogenesis) [5]. Thus, identification of the molecular mechanisms involved in skeletal muscle glucose metabolism should help clarify the pathophysiology of diabetes.

Nuclear receptors are part of a large superfamily of transcription factors that includes receptors for steroids, retinoic acid, and thyroid hormones [6]. RXRs are heterodimeric partners of many nuclear receptors, such as retinoic acid receptors (RARs), thyroid hormone receptors (T3Rs), liver X receptors (LXRs), peroxisome proliferator activated receptors (PPARs), and RXRs themselves [6]. Among RXR heterodimer partners, activation of PPARδ in the skeletal muscle increases insulin sensitivity [7]. The RXR subfamily consists of RXRα, RXRβ, and RXRγ [6,8]. Although RXRγ is preferentially expressed in the skeletal muscle, its functional role is poorly understood. We have recently found that expression of retinoid X receptor γ (RXRγ) is changed in the skeletal muscle under nutritional conditions; RXRγ mRNA expression is down-regulated by fasting and recovered by refeeding [9]. In an attempt to explore the role of RXRγ in the skeletal muscle, we established transgenic mice overexpressing RXRγ in the skeletal muscle (RXRγ mice) and found that they exhibit increased triglyceride contents in the skeletal muscle as a result of increased expression of sterol regulatory element binding protein 1c (SREBP1c), a transcriptional master regulator of lipogenesis [9]. Indeed, RXRγ has been shown to enhance SREBP1c gene expression in C2C12 myocytes *in vitro* at least in part by heterodimerization with LXR [9]. On the other hand, we also found that blood glucose levels are lower in RXRγ mice than in control mice [9]. These observations, taken together, suggest that RXRγ plays a critical role in glucose and lipid metabolism in the skeletal muscle. However, the molecular mechanism involved in RXRγ regulation of glucose metabolism in the skeletal muscle and how it affects systemic glucose metabolism are poorly understood.

Here, we demonstrate enhanced glucose metabolism with increased Glut1 expression and glucose uptake in RXRγ mice. This study suggests that activation of the skeletal muscle RXRγ is a novel therapeutic strategy to treat or prevent type 2 diabetes.

Methods

Animals

C57BL6 mice were purchased from Charles River Japan (Yokohama, Japan). Generation of RXRγ mice under the control of the human α-actin promoter was described previously [9]. They were allowed free access to food (CRF-1; Charles River) and water, unless otherwise stated. All animal experiments were approved by Institutional Animal Care and Use Committee of Tokyo Medical and Dental University (approval ID: No. 0090041).

Blood analysis

Serum samples were obtained from mice, when fed *ad libitum*. Serum glucose levels were measured by the blood glucose test meter (Glutest PRO R; Sanwa-Kagaku, Nagoya, Japan). Serum concentrations of insulin were determined by the enzyme-linked immunosorbent assay (ELISA) kits (Morinaga Institute of Biological Science, Inc., Yokohama, Japan).

Glucose and insulin tolerance tests

For glucose tolerance test, D-glucose (1 mg/g of body weight, 10% (w/v) glucose solution) was administered by intraperitoneal injection after an overnight fast. For insulin tolerance test, human insulin (Humulin R; Eli Lilly Japan K.K., Kobe, Japan) was injected intraperitoneally (0.75 mU/g of body weight), when fed *ad libitum*.

Hyperinsulinemic-euglycemic clamp studies

We analyzed as described previously [10–12] with slight modification. Two days before the clamp studies, a catheter was inserted into the right jugular vein for infusion under general anesthesia with sodium pentobarbital. Studies were performed on mice under conscious and unstressed conditions after a 4-h fast. The clamp study began with a prime (4 mg/kg for 5 min) of [6,6-^{2}H] glucose (Cambridge Isotope Laboratories, Inc, Andover, MA) followed by continuous infusion at a rate of 0.5 mg/kg per minute for 2 hr to assess the basal glucose turnover. After the basal period, hyperinsulinemic-euglycemic clamp was conducted for 120 min with a primed/continuous infusion of human insulin (25 mU/kg prime for 5 min, 5 mU/kg/min infusion) and variable infusion of 20% glucose to maintain euglycemia (approximately 100 mg/dl). The 20% glucose was enriched with [6,6-^{2}H] glucose to approximately 2.5% as previously described [12]. To determine the enrichment of [6,6-^{2}H]glucose in plasma at basal and insulin stimulated state, samples were deproteinized with trichloroacetic acid and derivatized with *p*-aminobenzoic acid ethyl ester. The atom percentage enrichment of glucose$_{m+2}$ was then measured by high-performance liquid chromatography with LTQ-XL-Orbitrap mass spectrometer (Thermo Scientific, CA). The glucose$_{m+2}$ enrichment was determined from the *m/z* ratio 332.2: 330.2. The hepatic glucose production was calculated by using the rate of infusion of [6,6-^{2}H]glucose over the atom percent excess in the plasma minus the rate of glucose being infused. The insulin-stimulated whole-body glucose uptake was calculated by adding the total glucose infusion rate plus the hepatic glucose production [12].

Quantitative real-time PCR. Quantitative real-time PCR was performed as described [9]. Total RNA was prepared using Sepazol (Nacalai Tesque, Kyoto, Japan). cDNA was synthesized from 5 μg of total RNA using Superscript II reverse transcriptase (Invitrogen Inc., Carlsbad, CA) with random primers. Gene expression levels were measured with an ABI PRISM 7700 using SYBR Green PCR Core Reagents (Applied Biosystems, Tokyo, Japan). The primers used were as follows, RXRγ: Fw: 5′-CAC-

Table 1. Body and dissected tissue weight and blood glucose level in RXRγ mice (4-3 line).

	Wild-type	RXRγ
Body weight (g)	26.4±0.3	26.5±0.4
Epididymal fat mass (g)	0.138±0.004	0.156±0.090
Gastrocnemius muscle weight (g)	0.282±0.004	0.238±0.008**
Liver weight (g)	1.290±0.029	1.321±0.033
Glucose (mg/dL) basal	170.0±9.4	145.6±4.9*
Glucose (mg/dL) fasting	74.4±1.7	67.0±0.6**

Mice were males 12 weeks of age. The number of animals used was 6 for both wild-type control and RXRγ mice.
* $P<0.05$;
** $P<0.01$, compared with wild-type control.
Values are the means ± SE. These samples were also used in Fig 2*A, B,* and *D*.
doi:10.1371/journal.pone.0020467.t001

Table 2. Body and dissected tissue weight and blood glucose level in RXRγ mice (5-3 line).

	Wild-type	RXRγ
Body weight (g)	36.0±1.8	31.9±1.2
Epididymal fat mass (g)	1.030±0.191	0.861±0.134
Gastrocnemius muscle weight (g)	0.305±0.016	0.214±0.020**
Liver weight (g)	1.375±0.119	1.320±0.066
Glucose (mg/dL) basal	142.5±8.6	117.3±8.2
Glucose (mg/dL) fasting	67.2±1.6	53.3±2.5**

Mice were males 38 weeks of age. The number of animals used was 6 for both wild-type control and RXRγ mice.
** $P<0.01$, compared with wild-type control.
Values are the means ± SE.
doi:10.1371/journal.pone.0020467.t002

CCTGGAGGCCTATACCA-3′, Rv: 5′-AAACCTGCCTGGCTGTTCC-3′, Glut1: Fw: 5′-CCAGC TGGGA ATCGT CGTT-3′, Rv: 5′-CAAGT CTGCA TTGCC CATGAT-3′, Glut4: Fw: 5′-TCTGTGGGTGGCATGATCTCT-3′, Rv: 5′-GCCCTTTTCCTTCCCAACC-3′, glucose phosphate isomerase 1: Fw: 5′-AGCGCTTCAACAACTTCAGCT-3′, Rv: 5′-CAGAATATGCCCATGGTTGGT-3′, phosphoglycerate mutase 1: Fw: 5′-TCCTGAAACATCTGGAAGGTATCTC-3′, Rv: 5′-CAGTGGGCAGAGTGATGTTGAT-3′, fructose bisphosphatase 2: Fw: 5′-TGAATGCAATCCTGTGGCC-3′, Rv: 5′-TGGTTGCCATACCTCCTGCT-3′, pyruvate dehydrogenase kinase isoenzyme 1: Fw: 5′-GGACTTCTATGCGCGCTTCT-3′, Rv: 5′-CTGACCCGAAGTCCAGGAAC-3′, glycogen synthase 2: Fw: 5′-AGGATCATTCAGAGGAACCGC-3′, Rv: 5′-CCAGTCCAGGAGATCTGAGAGC-3′.

Tissue sampling for analysis of Glut1 and Glut4 protein levels

Skeletal muscles were homogenized in ice-cold buffer containing 250 mmol/L sucrose, 20 mmol/L 2-[4-(2-hydroxyethyl)-1-piperadinyl] ethonsulforic acid (HEPES) (pH 7.4), and 1 mmol/L EDTA, and centrifuged at 1200 g for 5 minutes. The supernatant was centrifuged at 200 000 g for 60 minutes at 4°C [13]. The resulting pellet was solubilized in Laemmli sample buffer containing dithiothreitol. Samples were subjected to Western blotting as described [14]. Antibodies used were those against Glut1 (#07-1401, Millipore, Temecula, CA), and Glut4 (SC-1606, Santa Cruz Biotechnology Inc., Santa Cruz, CA).

Muscle incubation and glucose transport

Glucose transport was measured as described [15]. Mice were fasted overnight and killed. The extensor digitorum longus (EDL) muscles were rapidly removed, each of which was mounted on the incubation apparatus and preincubated in Krebs-Ringer bicarbonate (KRB) buffer containing 2 mmol/l pyruvate for 30 min. The muscles were then incubated in KRB buffer in the absence or presence of 50 mU/ml insulin for 10 min. The buffers were kept at 37°C throughout the experiment and gassed continuously with 95% O_2 and 5% CO_2. Immediately after incubation, the muscle was transferred to KRB buffer containing 1 mmol/l 2-[^{3}H]-deoxy-d-glucose (1.5 μCi/ml) and 7 mmol/l d-[^{14}C]-mannitol (0.3 μCi/ml).

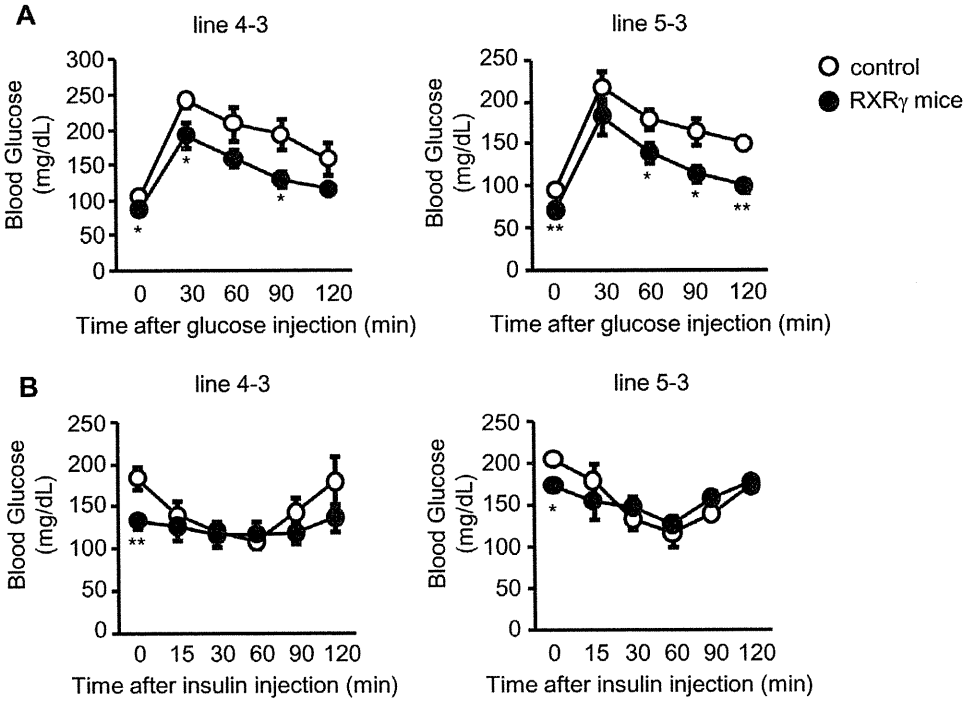

Figure 1. Glucose tolerance and insulin tolerance tests on RXRγ mice. (*A, B*) In A and B, male mice, 5 months of age, were used. The number of animals used was 6 for both control (open circles) and RXRγ (filled circles) mice of line 4-3, and 5 for both control (open circles) and RXRγ (filled circles) mice of line 5-3. * $P<0.05$ and ** $P<0.01$ compared with respective control.
doi:10.1371/journal.pone.0020467.g001

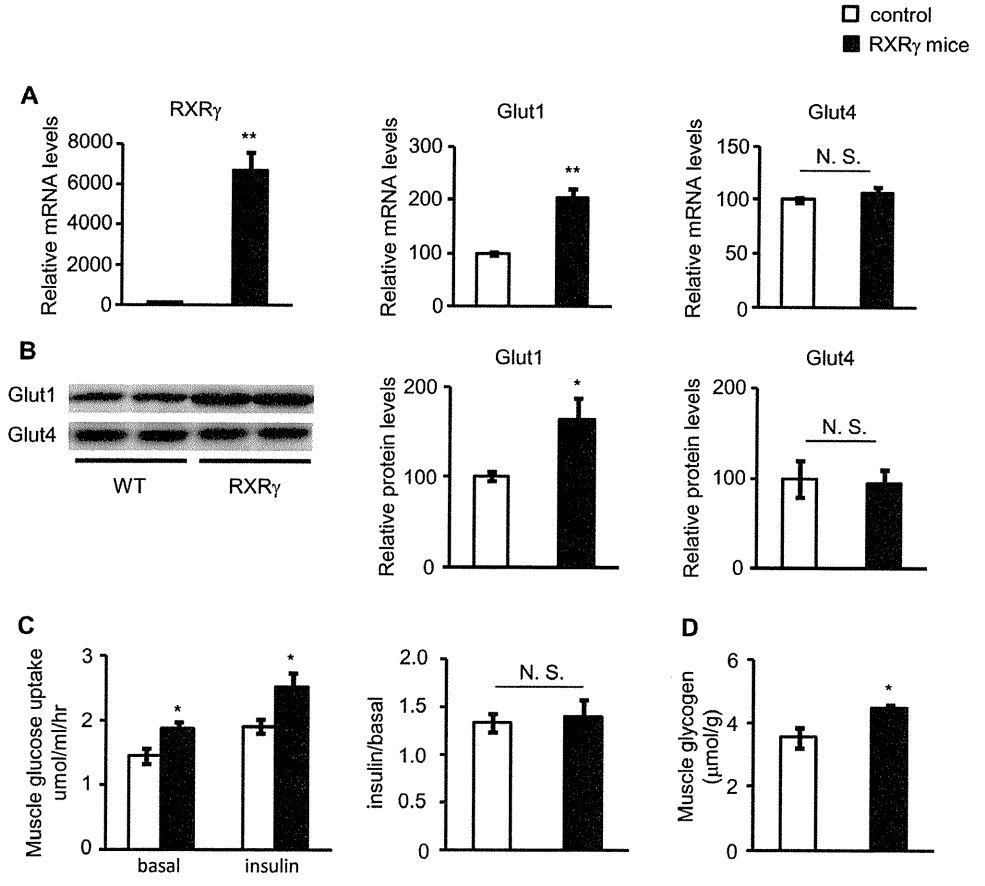

Figure 2. Levels of Glut 1 and Glut4, and glucose uptake in the skeletal muscle of RXRγ mice. (*A*) Gene expressions of *RXRγ*, *Glut1*, and *4* were examined by quantitative real-time PCR. The value for wild-type (littermates of line 4-3) mice was set at 100, and relative values are shown. (*B*) Protein levels of Glut1 and Glut4 were examined by Western blotting. Results of relative densitometric signal for Glut1 and 4 are shown. (*C*) Glucose uptake in the absence or presence of insulin and (*D*) glycogen content were increased in the skeletal muscle of RXRγ mice. Ratio of enhanced glucose uptake in the presence of insulin (insulin/basal) was similar in control and RXRγ mice. In *A*, *B* and *D*, the same samples were used. Mice were males of 12 weeks of age. The number of animals was 6 for both control (open bars) and RXRγ (filled bars) mice. These samples were also used in Table 1. In *C*, mice were males of 24–27 weeks of age. The number of animals was 6 for both control (open bars) and RXRγ (filled bars) mice. * $P<0.05$ and ** $P<0.01$ compared with respective control. N. S., not significant.
doi:10.1371/journal.pone.0020467.g002

Measurement of skeletal muscle glycogen

The skeletal muscle glycogen content was measured as glycosyl units after acid hydrolysis [16]. The skeletal muscle samples were minced, 50 mg of which was added to 1 ml of 0.3 M percholic acid and homogenized on ice. One ml of 1 N HCl was added and incubated for 2 h at 100°C, thereafter, 1 ml of 1 N NaOH was added at room temperature. Glucose content was examined using the F-kit glucose (Roche Diagnostics, Mannheim, Germany).

Plasmids

The coding region of mouse RXRγ and PPARδ cDNA were subcloned into a mammalian expression plasmid, pCMX [9]. The 1.5-kb 5′-flanking region of the mouse *Glut1* promoter was obtained by PCR with mouse genomic DNA (RefSeqs number: NC_000070). The PCR primers used were: Fw: 5′-GTGGTG-CGCGCCTGTAGTCC-3′ and Rv: 5′-GGCGCACTCCACG-GATGCCG-3′. The fragment was subcloned into the pGL3-basic luciferase vector (Promega Corporation, Madison, WI). The promoter regions used were: -1500 to +75, -647 to +75, and -152 to +75, counting the transcription start site as +1.

Electroporation and *in vivo* luciferase reporter analysis

In vivo electroporation was performed according to the modified method of Aihara and Miyazaki [17]. Under the pentobarbital anesthesia (30 mg/kg), bilateral quadriceps muscles from C57BL6

Table 3. Body weight, blood glucose and plasma insulin levels in RXRγ mice in clamp study.

		Wild-type	RXRγ
	Body weight (g)	24.1±1.2	23.4±0.3
Basal period	Glucose (mg/dL)	141.8±15.3	106.6±5.5*
	Insulin (ng/mL)	0.55±0.08	0.44±0.07
Clamp period	Glucose (mg/dL)	92.5±3.8	96.7±3.6
	Insulin (ng/mL)	2.60±0.20	2.38±0.33

Mice were males 13–16 weeks of age. The number of animals used was 6 for wild-type control mice and 7 for RXRγ mice.
* $P<0.05$, compared with wild-type control.
Values are the means ± SE. These mice were also used in Fig 3.
doi:10.1371/journal.pone.0020467.t003

mice (male, 12 weeks of age) were injected with 80 μg of plasmid DNA (25 μl) by using a 29-gauge needle attached to a 0.5-ml insulin syringe (Terumo Corporation, Tokyo, Japan). Square-wave electrical pulses (160 V/cm) were applied six times with an electrical pulse generator (CUY21EDIT, Nepa Gene Co. Ltd., Chiba, Japan) at a rate of one pulse per second, with each pulse being 20 ms. in duration. The electrodes were a pair of stainless steel needles inserted into the quadriceps muscles and fixed 5 mm apart. Seven days after gene delivery, the muscles were removed and subjected to analysis. Frozen muscle tissues were homogenized in ice-cold passive lysis buffer from Promega. The homogenate was centrifuged at 10,000 g for 10 min at 4°C. The supernatant was reserved for luciferase assay using Promega's dual luciferase assay kit. The luciferase activity was calculated as the ratio of firefly to Renilla (internal control) luciferase activity and represented as the average of triplicate experiments.

Computer-based DNA sequence motif search

We used MATCH software [18] (BIOBASE GmbH, Wolfenbuettel, Germany) to investigate transcriptional binding sites in the mouse *Glut1* promoter. We investigated mouse genome in the region of -1500 to +100 relative to transcription start of *Glut1* (Chr.4 11878131(+)).

cDNA microarray analysis

RNA was isolated from the skeletal muscle of sex- and age-matched RXRγ mice (line 4-3) and non-transgenic control mice

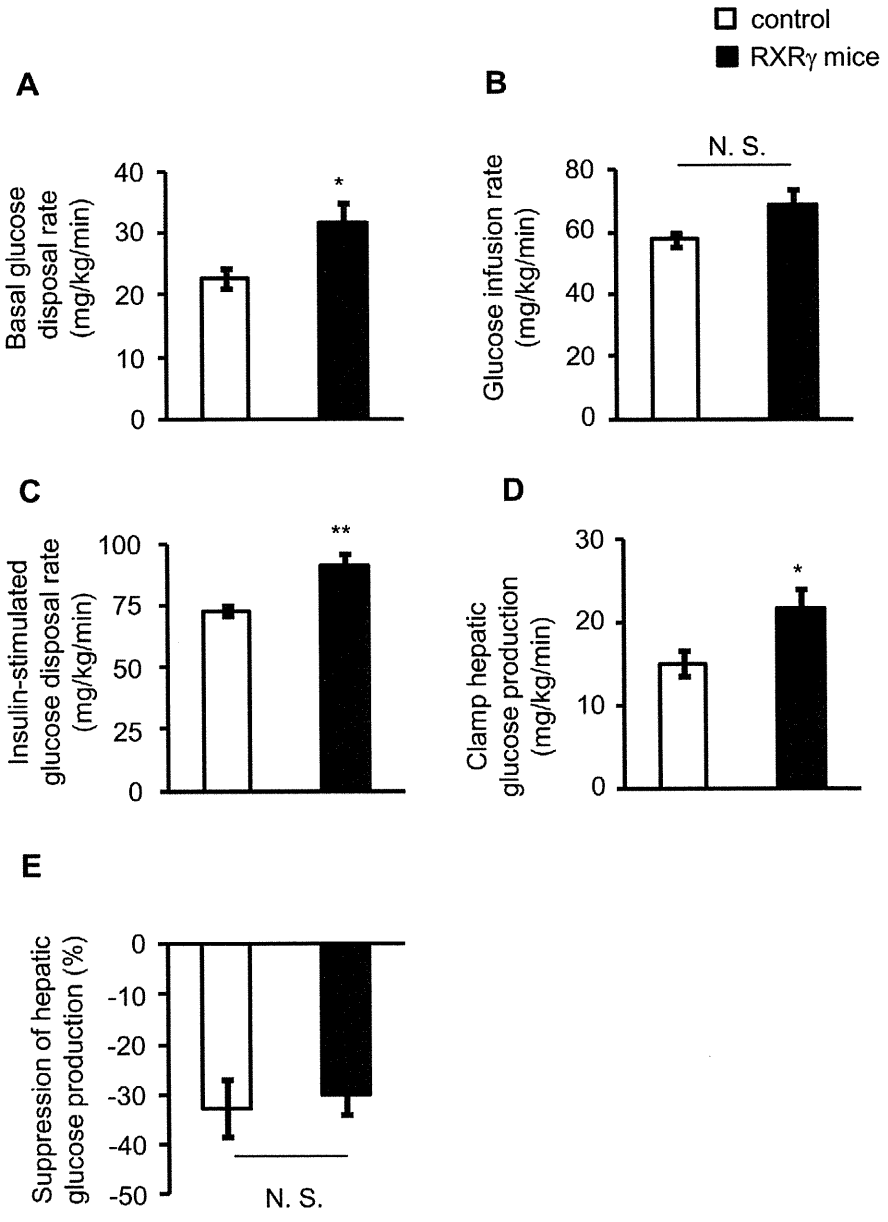

Figure 3. Hyperinsulinemic-euglycemic clamp test in RXRγ mice, fed a chow diet. (*A*) Basal glucose disposal rate, (*B*) glucose infusion rate needed to maintain euglycemia, (*C*) insulin-stimulated glucose disposal rate and (*D*) clamp hepatic glucose production (hepatic glucose production during the clamp period) (*E*) suppression of hepatic glucose production during the clamp period in RXRγ mice. Male mice, 13~16 weeks of age, were used. The number of animals used was 6 for control mice (open bars) and 7 for RXRγ mice (filled bars). * $P<0.05$ and ** $P<0.01$ compared with respective control. N. S., not significant.
doi:10.1371/journal.pone.0020467.g003

(females at 4 months of age, five samples from each group were combined). Each of the combined samples was hybridized to the Affymetrix MG430 microarray, which contains 45,102 genes, including expressed sequence tags (ESTs), and analyzed with the software Affymetrix Gene Chip 3.1. Of the 45,102 genes including ESTs analyzed, 8,054 (non-transgenic control mice) and 8,083 (transgenic) were expressed at a substantial level (absolute call is present and average difference is above 150). In order of fold changes in gene expression levels in skeletal muscle from RXRγ mice relative to control mice, genes whose expression was increased more than $2^{0.4}$-fold in RXRγ mice were listed (Dataset S1). Fold changes were calculated as an indication of the relative change of each transcript represented on the probe array. Differentially expressed genes were identified using the following criteria; 'absolute call' is present, and 'average difference' was above 250. 'Absolute call', which was calculated with this software using several markers, is an indicator of the presence or absence of each gene transcript. The 'average difference' value is a marker of the abundance of each gene, obtained by comparing the intensity of hybridization to 20 sets of perfectly matched 25-mer oligonucleotides relative to 20 sets of mismatched oligonucleotides using Affymetrix Gene Chip 3.1 software. All data of microarray is MIAME compliant and that the raw data has been deposited in a MIAME compliant database (GEO), whose accession number is GSE28448.

Gene Ontology Analysis

We used DAVID v6.7 [19] for gene ontology (GO) analysis. DAVID is a web application providing a comprehensive set of functional annotation tools to understand the biological meaning behind a large list of genes. Functional Annotation Clustering of DAVID was applied to the genes whose gene expression increased in RXRγ mice. Our GO analysis produced 62 GO terms from gene sets from RXRγ mice with increased expression compared to the wild-type mice, under the condition of $P<0.05$ (P value from Fisher's Exact Test). The obtained GO terms contained many similar functional concepts. In order to group similar GO terms, we applied the Functional Annotation Clustering tool provided by DAVID [19,20]. Twenty-three clusters were produced with genes showing increased expression. We showed one GO term of the lowest P value of all the members of an individual cluster.

Transcriptional factor binding sites analysis

We used MATCH software [18] with BKL TRANSFAC 2010.3 Release (BIOBASE GmbH, Worfenbuettel, Germany) to investigate transcriptional binding sites in the promoter regions of genes. The F-Match algorithm compares the number of sites found in a query sequence set against the background set. It is assumed, if a certain transcription factor (or factor family), alone or as a part of a *cis*-regulatory module, plays a significant role in the regulation of the considered set of promoters, then the frequency of the corresponding sites found in these sequences should be significantly higher than expected by random chance. We investigated the mouse genome in the region of -1000 to +100 relative to the transcription start of an individual gene. Statistical hypothesis testing was evaluated against housekeeping genes of mice. We investigated promoter regions of 15 genes: that is 14 'glucose metabolic process' genes with increased expression in RXRγ mice, plus Glut1. In the GO analysis, Glut1 was categorized as a 'transporter' not 'glucose metabolic process' gene.

Statistical analysis

Statistical analysis was performed using the Student's t test and analysis of variance (ANOVA) followed by Scheffe's test. Data were expressed as the mean ± SE. $P<0.05$ was considered statistically significant.

Results

Increased glucose metabolism in RXRγ mice

In our previous study, we established two lines of RXRγ mice (named lines 4-3 and 5-3) with similar expression levels of the *RXRγ* transgene and protein specifically in the skeletal muscle [9]. There was no significant difference in body weight, adipose tissue,

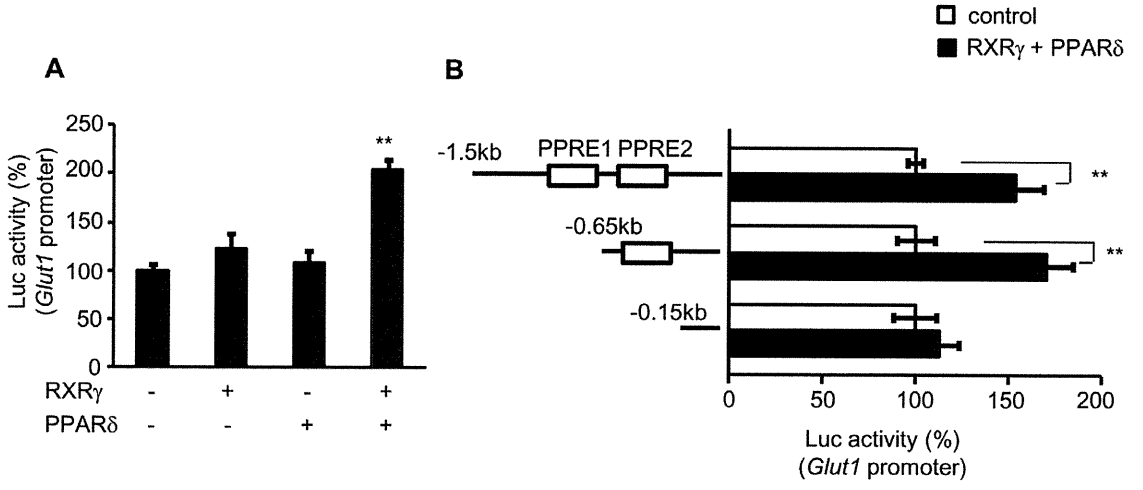

Figure 4. Transient transfection-reporter assay of the effect of RXRγ on *Glut1* promoter. (*A*) *Glut1*-Luc plasmid, with or without RXRγ and/or PPARδ expression vectors, was transfected into the quadriceps muscle of C57BL6 mice. Activation of the luciferase reporter gene was measured in relative light units and normalized to dual luciferase activity. Mean values from experiments (n = 5) are shown as fold induction, where the activity in the absence of RXRγ is the reference value (set at 100). (*B*) Schematic representations of serial deletion of *Glut1* promoter constructs are shown in the figure. Squares denote the putative PPAR/RXR binding sites. Open bars; *Glut1*-Luc without RXRγ and PPARδ expression vectors, and filled bars; *Glut1*-Luc with RXRγ and PPARδ expression vectors. The activity in the absence of RXRγ and PPARδ in each experiment for different *Glut1*-Luc construct in the reference value (set at 100). ** $P<0.01$, compared with the value of wild-type promoter in the absence of RXRγ/PPARδ.
doi:10.1371/journal.pone.0020467.g004

and liver weight between RXRγ and control mice in both lines 4-3 and 5-3, although the skeletal muscle weight was slightly lower in RXRγ mice than in control mice (Tables 1 and 2). In this study, blood glucose in RXRγ mice was lower than in control mice (fasting state, $P<0.01$ in lines 4-3 and 5-3; basal state, $P<0.05$ in line 4-3 and $P=0.06$ in line 5-3), which is consistent with our previous report [9].

To elucidate the role of the skeletal muscle RXRγ in systemic glucose metabolism, we performed glucose and insulin tolerance tests in RXRγ mice. The glucose tolerance test revealed increased glucose disposal in RXRγ mice relative to control mice (Fig. 1*A*). On the other hand, there was no significant difference in the insulin-induced hypoglycemic response between genotypes (Fig. 1*B*). These observations suggest that RXRγ mice have a higher capacity for glucose disposal with no change in insulin sensitivity.

Increased Glut1 expression and glucose uptake in the skeletal muscle of RXRγ mice

As both lines of RXRγ mice showed increased glucose metabolism, for the following experiments, we only utilized the line 4-3 of RXRγ mice (hereafter just RXRγ mice). Interestingly, mRNA expression of *Glut1* was increased in the skeletal muscle from RXRγ mice relative to control mice ($P<0.01$), whereas that of *Glut4* was unchanged (Fig. 2*A*). We also observed that Glut1 is significantly increased in RXRγ mice at the protein level ($P<0.05$), with no significant difference in Glut4 between genotypes (Fig. 2*B*). Consistently, we also found increased glucose uptake in the skeletal muscle from RXRγ mice relative to control mice ($P<0.05$), which was not further enhanced in the presence of insulin (Fig. 2*C*). We also observed increased glucose glycogen content in the skeletal muscle from RXRγ mice relative to control mice ($P<0.05$, Fig. 2*D*).

Table 4. Gene Ontology Analysis.

GO ID	GO Term	P value
GO:0060537	muscle tissue development	6.91E-05
GO:0006461	protein complex assembly	6.78E-05
GO:0008104	protein localization	1.18E-04
GO:0051146	striated muscle cell differentiation	6.06E-04
GO:0030334	regulation of cell migration	8.04E-04
GO:0006886	intracellular protein transport	0.002367379
GO:0019220	regulation of phosphate metabolic process	0.00312153
GO:0048514	blood vessel morphogenesis	0.00172443
GO:0045859	regulation of protein kinase activity	0.00563927
GO:0006915	apoptosis	0.007513423
GO:0006006	glucose metabolic process	0.002958786
GO:0006917	induction of apoptosis	0.005257921
GO:0042981	regulation of apoptosis	0.014518039
GO:0043066	negative regulation of apoptosis	0.022995692
GO:0006633	fatty acid biosynthetic process	0.012664127
GO:0032956	regulation of actin cytoskeleton organization	0.027565775
GO:0043388	positive regulation of DNA binding	0.021966247
GO:0006469	negative regulation of protein kinase activity	0.045894089
GO:0016477	cell migration	0.045248711
GO:0030521	androgen receptor signaling pathway	0.027402985
GO:0055003	cardiac myofibril assembly	0.020081231
GO:0000165	MAPKKK cascade	0.032045331
GO:0046825	regulation of protein export from nucleus	0.027402985

738 genes up-regulated in RXRγ mice compared with wild-type mice by microarray (Listed in Dataset S1) were classified into GO functional annotations, as described in Methods.
doi:10.1371/journal.pone.0020467.t004

Increased basal glucose disposal rate of RXRγ mice

To gain further insight into the glucose metabolism in RXRγ mice, we performed a hyperinsulinemic-euglycemic clamp study. Plasma insulin concentrations during the basal period were similar between genotypes (Table 3). The basal glucose disposal rate was significantly increased in RXRγ mice than in the controls ($P<0.05$, Fig. 3*A*), supporting that an insulin-independent increase in glucose uptake occurred, as observed in Fig. 2*C*. Meanwhile, we observed that the rate of glucose infusion needed to maintain euglycemia (glucose infusion rate) was similar between genotypes (Fig. 3*B*), which is consistent with the result of the insulin tolerance test (Fig. 1*B*). On the other hand, insulin-stimulated glucose disposal rate was higher in RXRγ mice than in the controls ($P<0.01$, Fig. 3*C*), which probably reflects the increased basal glucose disposal rate (Fig. 3*A*). Also, the clamp hepatic glucose production (hepatic glucose production during the clamp period) was higher in RXRγ mice than in the controls ($P<0.05$, Fig. 3*D*). Meanwhile, hepatic glucose production was similarly suppressed by insulin in both genotypes (Fig. 3*E*). Together, these data support the idea that Glut1, an insulin-independent glucose transporter, is involved in the increased glucose disposal in the skeletal muscle of RXRγ mice.

Activation of the *Glut1* promoter by combination of RXRγ and PPARδ in the skeletal muscle *in vivo*

To examine whether RXRγ directly activates mRNA expression of *Glut1*, we performed the *in vivo* luciferase reporter analysis

Table 5. List of 'glucose metabolic process' genes.

Gene Symbol	Gene description
Atf3	Activating transcription factor 3
Bpgm	2-3-bisphosphoglycerate mutase
Dcxr	Dicarbonyl L-xylulose reductase
Fbp2	Fructose bisphosphatase 2
Gbe1	Glucan branching enzyme 1
Gpd1l	Glycerol-3-phosphate dehydrogenase 1-like
Gpi1	Glucose phosphate isomerase 1
Gys2	Glycogen synthase 2
Igf2	Insulin-like growth factor 2
Mat2b	Methionine adenosyltransferase II, beta
Nisch	Nischarin; an imidazoline receptor
Pdk1	Pyruvate dehydrogenase kinase isoenzyme 1
Pgam1	Phosphoglycerate mutase 1
Pgd	Phosphogluconate dehydrogenase
Pgm2l1	Phosphoglucomutase 2-like 1
Phkb	Phosphorylase kinase beta

Up-regulated genes in RXRγ mice in the microarray, classified as 'glucose metabolic process' genes by GO analysis, as described in Method. Genes are listed in alphabetic order of gene symbol. Glut1, which appeared in the up-regulated list in the microarray (Dataset S1), is not included in this list, as it was classified 'transporter' in the GO analysis.
doi:10.1371/journal.pone.0020467.t005

using *Glut1* promoter (*Glut1*-Luc). In this study, the activity of *Glut1*-Luc was marginally enhanced by RXRγ alone (Fig. 4*A*). Moreover, we found no significant activation of the *Glut1*-Luc by PPARδ, an important regulator of glucose as well as lipid metabolism in the skeletal muscle [7]. Interestingly, combination of RXRγ and PPARδ resulted in significant increase in *Glut1*-Luc activity in the skeletal muscle *in vivo* ($P<0.01$) (Fig. 4*A*). Motif search analysis revealed two putative PPAR-responsive elements (PPRE1 and PPRE2) (−657/−645 and −520/−508, respectively) in the mouse *Glut1* promoter. A series of deletion mutant analysis showed that combination of RXRγ and PPARδ activates the regions of −1500/+75, and −647/+75, but not the region of −152/+75 in the *Glut1* promoter (Fig. 4*B*), suggesting that the second putative PPRE (−520/−508) is involved in the RXRγ/PPARδ-induced *Glut1* promoter activation.

Microarray and bioinformatics analyses of up-regulated gene in RXRγ mice

In order to gain insight into the gene expression change in RXRγ mice, we performed microarray analysis. As shown in Dataset S1, 738 genes were up-regulated in the analysis. As expected, Glut1 expression was increased in the microarray data. Also, SREBP1c expression, which we previously reported [9], was increased in the microarray data. Using the data, we performed GO analysis to determine if genes, up-regulated in RXRγ mice, are associated with particular biological processes. Our GO analysis revealed genes with increased expression in the RXRγ mice in various categories (Table 4), including 'glucose metabolic process' genes and 'fatty acid biosynthetic process' genes, which indicated that overexpression of RXRγ affects the expression of many genes. The up-regulated genes categorized as glucose metabolism genes in GO term are listed in Table 5. Among them, we confirmed enhanced gene expression by quantitative real time PCR (Fig. 5), supporting the microarray data reliable. Moreover, we calculated the ratio of putative transcription factor binding motifs in glucose metabolism genes, which were up-regulated in RXRγ mice. In the sample, several motifs showed statistical significance (Table 6) ($P<0.05$), including PPAR responsive elements. These data suggest that glucose metabolism genes up-regulated in RXRγ mice are possible target genes of the RXRγ and PPAR heterodimer.

Discussion

RXRγ is a nuclear receptor-type transcription factor that is expressed abundantly in the skeletal muscle and is regulated by nutritional conditions. Treatment of obese and diabetic mice with RXR pan-agonists (agonists for all the RXR isoforms) has improved glucose metabolism in mice [21–23], suggesting the beneficial effect of RXR on diabetes. However, which RXR isoform(s) are involved and where they work to improve diabetes

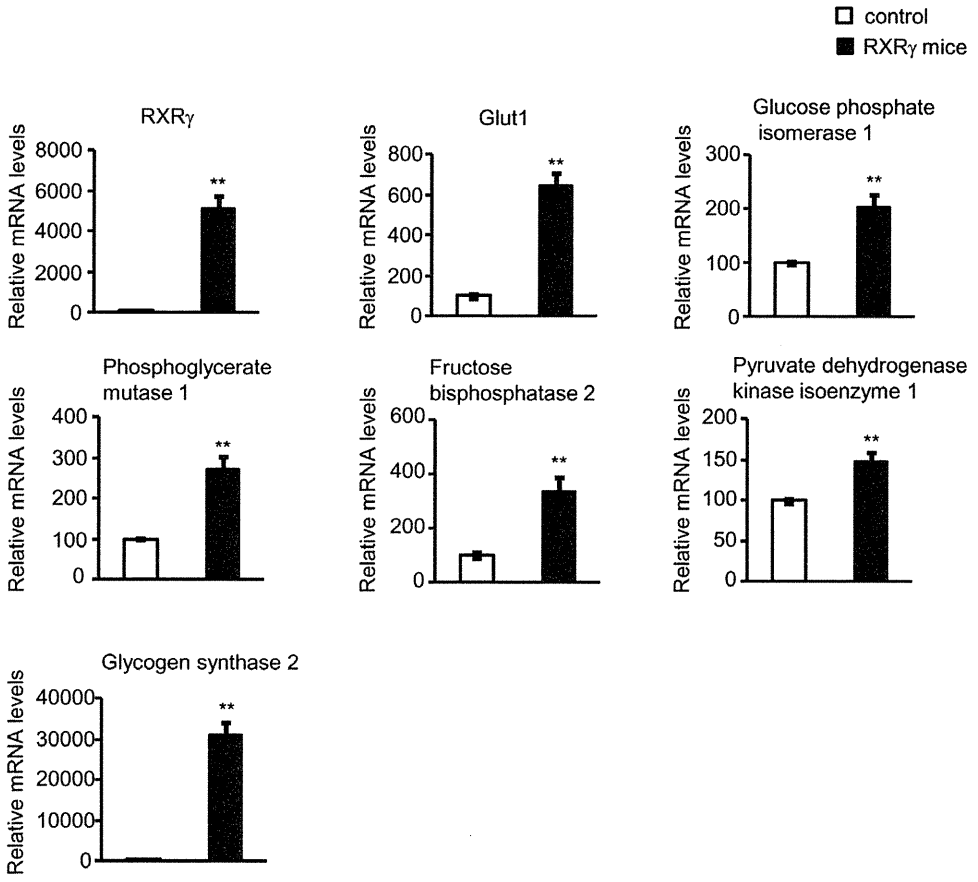

Figure 5. Levels of 'glucose metabolic process' gene expression in the skeletal muscle of RXRγ mice. Representative gene expressions of 'glucose metabolic process genes' analyzed by microarray and GO analysis (Table 5) were examined by quantitative real-time PCR. The value for wild-type (littermates of line 4-3) mice was set at 100, and relative values are shown. Mice were females of 4 months of age. The number of animals was 6 for both control (open bars) and RXRγ (filled bars) mice. These samples were also used in microarray analysis (Dataset S1). * $P<0.05$ and ** $P<0.01$ compared with respective control. N. S., not significant.
doi:10.1371/journal.pone.0020467.g005

Table 6. Possible transcription factor binding sites in the 'glucose metabolic process' gene up-regulated in RXRγ mice.

Transcription factors	Matrix name	P-value
WT1, WT1 -KTS, WT1 I, WT1 I -KTS	WT1_Q6	6.98E-04
HNF-4, HNF-4alpha	HNF4ALPHA_Q6	0.0013
PPARalpha	PPARA_01	0.0017
c-Myb, c-Myb-isoform1	VMYB_02	0.0026
PPARalpha, PPARdelta, PPARgamma	PPAR_DR1_Q2	0.003
CART1, CART1, CART1	CART1_01	0.0036
COUP-TF1, COUP-TF2, HNF-4, HNF-4alpha	COUP_DR1_Q6	0.0036
CP2, CP2-isoform1	CP2_02	0.0055
NRF1-isoform1, NRF1-isoform2, NRF1-xbb1	TCF11_01	0.0057
SZF1	SZF11_01	0.0057
PPARgamma	PPARG_01	0.0057
COUP-TF1, COUP-TF2, HNF-4, HNF-4alpha, HNF4gamma	DR1_Q3	0.0057
BRCA1, BRCA1	BRCA_01	0.0065
HNF-3beta	HNF3B_01	0.007
Pax-2b, pax2	PAX2_01	0.007
C/EBPalpha, C/EBPbeta(LAP), C/EBPbeta(p20), C/EBPbeta(p20), C/EBPbeta(p34), C/EBPbeta(p35), C/EBPgamma, cebpe, CRP3, NF-IL6-1, NF-IL6-3	CEBP_Q3	0.007
MITF, MITF-M1, tcfec, TFEA, TFEA-xbb1, TFEA-xbb2, tfeb, tfeb-isoform1	TFE_Q6	0.007
AP-2alpha, AP-2beta, AP-2gamma	AP2_Q6_01	0.0077
Pax-4a, Pax-4c, Pax-4d, Pax4	PAX4_04	0.0079
c-Myc, deltaMax, max, max-isoform1, max-isoform2, N-Myc	MYCMAX_03	0.0093

The mouse genome in the region of −1000 to +100 relative to the transcription start of an individual gene classified as glucose metabolism gene by GO analysis (Table 5), was analyzed. Statistical hypothesis testing was evaluated against housekeeping genes of mice. Matrics names are based on the MATCH software (see **Methods**), which are listed in *P*-value order. Indicated binding sites of transcription factors appeared significantly more frequent occurrence in the promoter sets.
doi:10.1371/journal.pone.0020467.t006

has not been addressed. Here, we investigated glucose metabolism in RXRγ mice.

We demonstrated increased glucose metabolism in RXRγ mice relative to control mice, although there was no significant difference in the insulin-induced hypoglycemic effect between genotypes, based on insulin tolerance test and glucose clamp analysis. Because insulin level is similar between RXRγ mice and control mice, it is unlikely that increased insulin secretion is responsible for increased glucose tolerance in RXRγ mice. On the other hand, mRNA and protein expression of Glut1 is increased in the skeletal muscle from RXRγ mice relative to control mice, with increased glucose uptake and glycogen content. Because transgenic overexpression of Glut1 in the skeletal muscle has resulted in increased glucose uptake [24], glycogen content [25] and lowering of blood glucose [24], it is likely that enhanced glucose tolerance in RXRγ mice is mediated at least in part by increased Glut1 in the skeletal muscle.

As RXRγ is a nuclear receptor-type transcription factor that heterodimerizes with many nuclear receptors [6], we examined whether the *Glut1* gene is directly regulated by RXRγ. In an *in vivo* luciferase reporter analysis, combination of RXRγ and PPARδ activates the *Glut1* promoter activity, which is diminished by deletion of the putative PPREs. It is, therefore, RXRγ/PPARδ may activate *Glut1* expression in the skeletal muscle *in vivo*. In this regard, we found that overexpression of RXRγ or PPARδ alone or both in C2C12 myocytes *in vitro* does not induce *Glut1* gene expression (unpublished data). This may be because C2C12 cells lack other factor(s) that are present in the skeletal muscle *in vitro* and are required to activate *Glut1* transcription. Whether the increased *Glut1* gene in RXRγ mice is mediated by RXRγ/PPARδ should be confirmed by additional experiments using PPARδ knockout mice. Meanwhile, the transgene expression level in RXRγ mice was very high, and appeared to be beyond the physiological level. Nonetheless, if RXRγ can be enhanced in skeletal muscle, an increase in glucose metabolism can be expected.

We recently demonstrated that in addition to glycogen content, RXRγ mice exhibit increased triglyceride in the skeletal muscle as a result of increased SREBP1c gene expression [9]. In obese and diabetic subjects, intramuscular lipid is high with insulin resistance [26]. Moreover, in athletes, the skeletal muscle is also high in lipid but with high insulin sensitivity, which is known as the athlete paradox [27,28]. A partial explanation is an increased fatty acid load in obese and diabetic subjects, but not in athletes; increased intramuscular lipotoxic fatty acid metabolites, such as diacylglycerol and ceramide, cause insulin resistance in skeletal muscles [29,30]. Taken together with our previous report [9], this study demonstrates that RXRγ mice do not develop insulin resistance despite high intramuscular lipids, and appear to be protected against obesity-induced lipotoxicity in the skeletal muscle. Depositing glucose as both glycogen and triglycerides in the skeletal muscle may be effective in enhancing glucose metabolism.

Microarray analysis showed that various genes are up-regulated in the skeletal muscle of RXRγ mice. As RXRγ can heterodimerize several nuclear receptors, it is not surprising that expression of many genes was up-regulated by RXRγ overexpression. Concerning glucose metabolism genes, in the skeletal muscle of RXRγ mice, the expression levels of genes, such as glucose phosphate isomerase 1 and phosphoglycerate mutase 1 (stimulate glycolysis or gluconeogenesis), fructose bisphosphatase 2 (stimulates gluconeogenesis), pyruvate dehydrogenase kinase

isoenzyme 1 (suppresses glycolysis), glycogen synthase 2 (stimulates glycogen synthesis)[31,32], were markedly increased (Fig. 5), suggesting the anabolic reaction of glucose. This is consistent with the observation that the glycogen content of skeletal muscle is higher in RXRγ mice (Fig. 2C). It is of note that glycogen synthase 2 is a liver-type enzyme, not a skeletal muscle-type enzyme [32]. In addition, usually, gluconeogenesis is not considered to be a major metabolic pathway in skeletal muscle. Chronic transgenic overexpression of RXRγ may have caused a super-physiological gene expression change in the skeletal muscle. Meanwhile, our bioinformatics analysis showed that glucose metabolism genes up-regulated in RXRγ mice contain several transcription factor binding motifs including PPRE in their promoter region. These observations support the concept that the RXRγ/PPAR heterodimer contributes to activation of these gene sets, although this needs to be confirmed by further experiments.

In summary, we demonstrated enhanced glucose metabolism with increased Glut1 expression and glucose uptake in RXRγ mice. This study suggested that activation of the skeletal muscle RXRγ is a novel therapeutic strategy to treat or prevent type 2 diabetes.

Supporting Information

Dataset S1 List of genes up-regulated in RXRγ mice compared with wild-type control mice by microarray.
(XLS)

Acknowledgments

We thank Dr. Christopher K. Glass (University of California, San Diego) for discussion. We thank Dr. Kotaro Ishibashi (Daiichi-Sankyo Co., Ltd.) for assistance in animal experiments.

Author Contributions

Conceived and designed the experiments: JIO KN SS YK OE YO. Performed the experiments: SS YK FA TS SK (Sayaka Kanai) MH YM NF TTI MT HA TY HK (Hideki Katagiri) SK (Saori Kakehi) YT HK (Hideo Kubo) SM. Analyzed the data: SS YK FA TS SK (Sayaka Kanai) MH YM NF TTI HA TY HK (Hideki Katagiri) SK (Saori Kakehi) YT HK (Hideo Kubo) SM. Contributed reagents/materials/analysis tools: TTI HA JIO KN. Wrote the paper: SS YK OE YO.

References

1. Zurlo F, Larson K, Bogardus C, Ravussin E (1990) Skeletal muscle metabolism is a major determinant of resting energy expenditure. J Clin Invest 86: 1423–1427.
2. DeFronzo RA (1988) Lilly lecture 1987. The triumvirate: beta-cell, muscle, liver. A collusion responsible for NIDDM. Diabetes 37: 667–687.
3. Marshall BA, Hansen PA, Ensor NJ, Ogden MA, Mueckler M (1999) GLUT-1 or GLUT-4 transgenes in obese mice improve glucose tolerance but do not prevent insulin resistance. Am J Physiol 276: E390–E400.
4. Petersen KF, Dufour S, Savage DB, Bilz S, Solomon G, et al. (2007) The role of skeletal muscle insulin resistance in the pathogenesis of the metabolic syndrome. Proc Natl Acad Sci U S A 104: 12587–12594.
5. Kim JK, Zisman A, Fillmore JJ, Peroni OD, Kotani K, et al. (2001) Glucose toxicity and the development of diabetes in mice with muscle-specific inactivation of GLUT4. J Clin Invest 108: 153–160.
6. Shulman AI, Mangelsdorf DJ (2005) Retinoid x receptor heterodimers in the metabolic syndrome. N Engl J Med 353: 604–615.
7. Lee CH, Olson P, Hevener A, Mehl I, Chong LW, et al. (2006) PPARdelta regulates glucose metabolism and insulin sensitivity. Proc Natl Acad Sci U S A 103: 3444–3449.
8. Szanto A, Narkar V, Shen Q, Uray IP, Davies PJ, et al. (2004) Retinoid X receptors: X-ploring their (patho)physiological functions. Cell Death Differ 11: S126–S143.
9. Kamei Y, Miura S, Suganami T, Akaike F, Kanai S, et al. (2008) Regulation of SREBP1c gene expression in skeletal muscle: role of retinoid X receptor/liver X receptor and forkhead-O1 transcription factor. Endocrinology 149: 2293–2305.
10. Suzuki R, Tobe K, Aoyama M, Inoue A, Sakamoto K, et al. (2004) Both insulin signaling defects in the liver and obesity contribute to insulin resistance and cause diabetes in Irs2(-/-) mice. J Biol Chem 279: 25039–25049.
11. Uno K, Katagiri H, Yamada T, Ishigaki Y, Ogihara T, et al. (2006) Neuronal pathway from the liver modulates energy expenditure and systemic insulin sensitivity. Science 312: 1656–1659.
12. Erion DM, Yonemitsu S, Nie Y, Nagai Y, Gillum MP, et al. (2009) SirT1 knockdown in liver decreases basal hepatic glucose production and increases hepatic insulin responsiveness in diabetic rats. Proc Natl Acad Sci U S A 106: 11288–11293.
13. Tanaka S, Hayashi T, Toyoda T, Hamada T, Shimizu Y, et al. (2007) High-fat diet impairs the effects of a single bout of endurance exercise on glucose transport and insulin sensitivity in rat skeletal muscle. Metabolism 56: 1719–1728.
14. Ito A, Suganami T, Miyamoto Y, Yoshimasa Y, Takeya M, et al. (2007) Role of MAPK phosphatase-1 in the induction of monocyte chemoattractant protein-1 during the course of adipocyte hypertrophy. J Biol Chem 282: 25445–25452.
15. Fujii N, Ho RC, Manabe Y, Jessen N, Toyoda T, et al. (2008) Ablation of AMP-activated protein kinase alpha2 activity exacerbates insulin resistance induced by high-fat feeding of mice. Diabetes 57: 2958–2966.
16. Lowry OH, Passonneau JV (1972) A flexible system of enzymatic analysis. Academic Press London 1-291.
17. Aihara H, Miyazaki J (1998) Gene transfer into muscle by electroporation in vivo. Nat Biotechnol 16: 867–870.
18. Kel AE, Gossling E, Reuter I, Cheremushkin E, Kel-Margoulis OV, et al. (2003) MATCH: A tool for searching transcription factor binding sites in DNA sequences. Nucleic Acids Res 31: 3576–3579.
19. Huang da W, Sherman BT, Lempicki RA (2009) Systematic and integrative analysis of large gene lists using DAVID bioinformatics resources. Nat Protoc 4: 44–57.
20. Carbon S, Ireland A, Mungall CJ, Shu S, Marshall B, Lewis S (2009) AmiGO: online access to ontology and annotation data. Bioinformatics 25: 288–289.
21. Mukherjee R, Davies PJ, Crombie DL, Bischoff ED, Cesario RM, et al. (1997) Sensitization of diabetic and obese mice to insulin by retinoid X receptor agonists. Nature 386: 407–410.
22. Davies PJ, Berry SA, Shipley GL, Eckel RH, Hennuyer N, et al. (2001) Metabolic effects of rexinoids: tissue-specific regulation of lipoprotein lipase activity. Mol Pharmacol 59: 170–176.
23. Shen Q, Cline GW, Shulman GI, Leibowitz MD, Davies PJ (2004) Effects of rexinoids on glucose transport and insulin-mediated signaling in skeletal muscles of diabetic (db/db) mice. J Biol Chem 279: 19721–19731.
24. Marshall BA, Ren JM, Johnson DW, Gibbs EM, Lillquist JS, et al. (1993) Germline manipulation of glucose homeostasis via alteration of glucose transporter levels in skeletal muscle. J Biol Chem 268: 18442–18445.
25. Ren JM, Marshall BA, Gulve EA, Gao J, Johnson DW, et al. (1993) Evidence from transgenic mice that glucose transport is rate-limiting for glycogen deposition and glycolysis in skeletal muscle. J Biol Chem 268: 16113–16115.
26. Goodpaster BH, Wolf D (2004) Skeletal muscle lipid accumulation in obesity, insulin resistance, and type 2 diabetes. Pediatr Diabetes 5: 219–226.
27. Stannard SR, Johnson NA (2004) Insulin resistance and elevated triglyceride in muscle: more important for survival than "thrifty" genes? J Physiol 554: 595–607.
28. Goodpaster BH, He J, Watkins S, Kelley DE (2001) Skeletal muscle lipid content and insulin resistance: evidence for a paradox in endurance-trained athletes. J Clin Endocrinol Metab 86: 5755–5761.
29. Schenk S, Horowitz JF (2007) Acute exercise increases triglyceride synthesis in skeletal muscle and prevents fatty acid-induced insulin resistance. J Clin Invest 117: 1690–1698.
30. Liu L, Zhang Y, Chen N, Shi X, Tsang B, et al. (2007) Upregulation of myocellular DGAT1 augments triglyceride synthesis in skeletal muscle and protects against fat-induced insulin resistance. J Clin Invest 117: 1679–1689.
31. Kaslow HR, Lesikar DD, Antwi D, Tan AW (1985) L-type glycogen synthase. Tissue distribution and electrophoretic mobility. J Biol Chem 260: 9953–9956.
32. Salway JG (1999) Metabolism at a glance. London: Blackwell Science Ltd.

Circulation
JOURNAL OF THE AMERICAN HEART ASSOCIATION

American Heart Association®
Learn and Live℠

Involvement of Endoplasmic Stress Protein C/EBP Homologous Protein in Arteriosclerosis Acceleration With Augmented Biological Stress Responses

Junhong Gao, Yasushi Ishigaki, Tetsuya Yamada, Keiichi Kondo, Suguru Yamaguchi, Junta Imai, Kenji Uno, Yutaka Hasegawa, Shojiro Sawada, Hisamitsu Ishihara, Seiichi Oyadomari, Masataka Mori, Yoshitomo Oka and Hideki Katagiri

Circulation published online August 1, 2011
Circulation is published by the American Heart Association. 7272 Greenville Avenue, Dallas, TX 72514
 Print ISSN: 0009-7322. Online ISSN: 1524-4539

Involvement of Endoplasmic Stress Protein C/EBP Homologous Protein in Arteriosclerosis Acceleration With Augmented Biological Stress Responses

Junhong Gao, MD, PhD; Yasushi Ishigaki, MD, PhD; Tetsuya Yamada, MD, PhD; Keiichi Kondo, MD; Suguru Yamaguchi, MD, PhD; Junta Imai, MD, PhD; Kenji Uno, MD, PhD; Yutaka Hasegawa, MD, PhD; Shojiro Sawada, MD, PhD; Hisamitsu Ishihara, MD, PhD; Seiichi Oyadomari, MD, PhD; Masataka Mori, MD, PhD; Yoshitomo Oka, MD, PhD; Hideki Katagiri, MD, PhD

Background—The processes of arteriosclerosis, including atherosclerosis and vascular remodeling, are affected by interactions among numerous biological pathways such as responses to inflammation, oxidative stress, and endoplasmic reticulum stress. C/EBP homologous protein (CHOP), which is well known to induce cellular apoptosis in response to severe endoplasmic reticulum stress, is reportedly upregulated in plaque lesions.

Methods and Results—We examined the effects of CHOP deficiency on 2 types of arteriosclerosis: cuff injury–induced neointimal formation and hypercholesterolemia-induced atherosclerosis. Cuff injury–induced neointimal formation was markedly inhibited in $CHOP^{-/-}$ mice with suppressed aortic expression of inflammatory factors and smooth muscle cell proliferation–related proteins. A CHOP deficiency also inhibited aortic plaque formation in hypercholesterolemic apolipoprotein $E^{-/-}$ mice with suppressed aortic expression of inflammatory factors and oxidative stress markers. Bone marrow transplantation experiments revealed that recipient CHOP deficiency significantly suppressed both cuff injury–induced neointimal formation and hypercholesterolemia-induced atherosclerotic plaque formation to a greater extent than donor CHOP deficiency, suggesting the importance of CHOP in vascular cells for arteriosclerosis progression. Furthermore, in our in vitro experiments, in not only macrophages but also endothelial and smooth muscle cell lines, endoplasmic reticulum stress inducers upregulated inflammation-, adhesion-, or smooth muscle cell proliferation–related proteins, whereas decreased CHOP expression remarkably suppressed endoplasmic reticulum stress–induced upregulation of these proteins.

Conclusions—In addition to the well-known signaling for apoptosis induction, CHOP may play important roles in augmenting potentially pathological biological stress responses. This noncanonical role of CHOP, especially that expressed in vascular cells, may contribute to the progression of vascular remodeling and atherosclerosis. **(*Circulation*. 2011;124:830-839.)**

Key Words: atherosclerosis ■ inflammation ■ remodeling ■ stress, physiological ■ transcription factor CHOP

The mechanisms underlying the pathogenesis of arteriosclerosis such as vascular remodeling and atherosclerosis development are extremely complex and are affected by interactions among numerous biological pathways, including those of inflammation,[1] metabolic disorders,[2] and oxidative stress.[3] Oxidized low-density lipoprotein (LDL) is proposed to play a central role in hypercholesterolemia-induced atherosclerotic development,[4] not only through its incorporation into macrophages to form foam cells but also through the promotion of inflammatory cytokine release and oxidative stress in vascular walls.[5] In addition to inflammation and oxidative stress, several lines of evidence have suggested exacerbation of endoplasmic reticulum (ER) stress in atherosclerotic lesions.

Clinical Perspective on p 839

The ER is an organelle that has essential roles in multiple cellular processes required for cell survival and normal cellular functions. Various disturbances, including ischemia, hypoxia, oxidative injury, and viral infections, trigger protein unfolding in the ER, leading to unfolded protein responses (UPRs), also known as ER stress responses.[6] Recent studies have revealed that ER stress is associated with a wide range of diseases, including neurodegenerative disorders,[7] cancer,[8] and diabetes

Received February 21, 2010; accepted June 7, 2011.

From the Department of Metabolic Diseases, Center for Metabolic Diseases (J.G., T.Y., K.K., K.U., H.K.) and Division of Molecular Metabolism and Diabetes (Y.I., K.K., S.Y., J.I., Y.H., S.S., H.I., Y.O.), Tohoku University Graduate School of Medicine, Sendai; Division of Molecular Biology, Institute for Genome Research, University of Tokushima, Tokushima (S.O.); and Laboratory of Molecular Genetics, Faculty of Pharmaceutical Sciences, Sojo University, Kumamoto (M.M.), Japan.

The online-only Data Supplement is available with this article at http://circ.ahajournals.org/lookup/suppl/doi:10.1161/CIRCULATIONAHA.110.014050/-/DC1.

Correspondence to Hideki Katagiri, MD, PhD, Department of Metabolic Diseases, Center for Metabolic Diseases, Tohoku University Graduate School of Medicine, 2-1 Seiryo-machi, Aoba-ku, Sendai 980-8575, Japan. E-mail katagiri@med.tohoku.ac.jp

Circulation **is available at http://circ.ahajournals.org** **DOI: 10.1161/CIRCULATIONAHA.110.014050**

mellitus.[9] In terms of atherosclerosis development, ER stress is reportedly increased in atherosclerotic lesions of apolipoprotein E (apoE)–deficient mice.[10] Free cholesterol incorporated into macrophages induces ER stress, leading to macrophage apoptosis.[11] In addition, ER stress is involved in oxidized LDL–induced endothelial dysfunction.[12] Endoplasmic reticulum stress in the vascular wall may exacerbate oxidative stress and inflammation.[13,14] In human subjects, ER stress in atherosclerotic plaques could be associated with acute coronary syndrome.[15] Collectively, these findings suggest that ER stress plays important roles in atherosclerosis development.

The UPR is an adaptive response that first tends to restore ER activity and cellular homeostasis but switches toward apoptosis when ER stress is severe or prolonged. The transcription factor C/EBP homologous protein (CHOP; also known as GADD153) is a downstream component of ER stress pathways and induces cellular apoptosis.[16] It is highly expressed in atherosclerotic plaque lesions.[10] Thorp and colleagues reported that CHOP deficiency suppressed atherosclerotic progression in apoE$^{-/-}$ mice via a mechanism involving decreased atherosclerotic plaque necrosis and lesional apoptosis of macrophages.[17] In addition to induction of apoptosis, CHOP can exacerbate ER stress by inducing the expression of genes encoding ER client proteins such as GADD34 and by rendering the ER more oxidative by inducing expression of ER oxidase 1 (ERO1α).[18–20] These findings prompted us to hypothesize that CHOP is a key molecule linking several biological stress responses and thereby accelerates arteriosclerosis development. Therefore, we analyzed the roles of CHOP, especially that expressed in vascular cells, in these biological responses and the resultant arteriosclerotic processes such as vascular remodeling and atherosclerosis.

Methods

Animals

Animal studies were conducted in accordance with the institutional guidelines for animal experiments at Tohoku University. The CHOP$^{-/-}$ mice[21] were backcrossed for at least 8 generations with C57BL/6J mice (Nippon CLEA, Shizuoka, Japan). The CHOP$^{-/-}$ mice were mated with female apoE$^{-/-}$ mice[22] (The Jackson Laboratory, Bar Harbor, ME) to establish a line of CHOP$^{-/-}$;apoE$^{-/-}$ mice. To accelerate the development of atherosclerosis, these mice were fed a 1.25% high-cholesterol diet[23] from 8 weeks of age.

Plasma Metabolic Parameters

Blood glucose, plasma adiponectin, and tumor necrosis factor-α levels and serum total cholesterol, triglyceride, and free fatty acid concentrations were determined as described previously.[24] Plasma levels of monocyte chemoattractant protein-1 (MCP-1), malondialdehyde, and 8-isoprostane were measured with an ELISA kit (R&D Systems, Minneapolis, MN), a TBARS Assay kit (Cayman Chemical Company, Ann Arbor, MI), and an 8-isoprostane enzyme immunoassay kit (Cayman Chemical Company), respectively.

Blood Pressure Determinations

Systolic blood pressures were measured over several days in conscious mice with a tail-cuff system (Muromachikikai Co, Kyoto, Japan) according to the manufacturer's instructions. Five to 8 measurements were recorded for each mouse. Results are presented as the mean of measurements on consecutive days.

Cuff Injury of Femoral Arteries

Polyethylene PE-50 tubes (2 mm; inner diameter, 0.58 mm; outer diameter, 0.965 mm; Becton Dickinson, Franklin Lakes, NJ) were placed around the right femoral arteries of 8-week-old mice as described previously.[25] The contralateral artery served as an uninjured control. Vessels were isolated and processed for histological analyses 3 weeks after cuff placement. The middle segment of the artery was cut at 50-μm intervals, and the thicknesses of the intima and media were measured.

Quantitative Reverse-Transcription Polymerase Chain Reaction-Based Gene Expression

Quantitative reverse-transcription polymerase chain reaction was performed as previously described.[26] The relative amount of mRNA was calculated with α-actin mRNA for cuff injury experiments or with GAPDH mRNA for the apoE$^{-/-}$ mouse and in vitro experiments as the invariant control. The oligonucleotide primers are described in Table I in the online-only Data Supplement.

Immunoblotting

Immunoblot analyses were performed as previously described[4] using antibodies to Bip (GRP78) (Santa Cruz Biotechnology, Santa Cruz, CA), mouse class A type I scavenger receptor (R&D Systems, Inc), and GAPDH (Ambion, Austin, TX).

Evaluation of Atherosclerotic Lesions

The atherosclerotic lesions were evaluated as Oil Red O–stained areas, as described previously.[4] The aortas were removed, cleaned, cut open with the luminal surface facing up, and then immersion fixed in 10% formalin in PBS. The inner aortic surfaces were stained with Oil Red O for 30 minutes at room temperature. The Oil Red O–stained areas were quantified by Scion Image software analysis (Scion Corp, Frederick, MD) of the digitized microscopic images. For aortic root cross-section analyses, the aortic root and ascending aorta were excised from mice, rinsed in normal saline, and frozen in optimal cutting temperature compound (Sakura Finetek, Tokyo, Japan). The sections were stained with Oil Red O and counterstained with hematoxylin and eosin.

Tissue Collection and Immunohistochemical Staining

Aortas were snap-frozen in liquid nitrogen, stored at −80°C for protein and gene expression studies, and then embedded in optimum cutting temperature compound.[27] The proximal artery was cut into subserial 6-μm cross sections and stained with antibodies to oxidized LDL (Calbiochem, San Diego, CA), MOMA-2 (Serotec, Oxford, UK), α-smooth muscle actin (Progen, Heidelberg, Germany), and proliferating cell nuclear antigen (Santa Cruz Biotechnology).

Irradiation and Bone Marrow Transplantation

The CHOP$^{+/+}$ and CHOP$^{-/-}$ recipient mice underwent lethal irradiation (10 Gy) at 6 weeks of age and then received 4×10^6 freshly prepared sterile bone marrow cells obtained from CHOP$^{+/+}$ and CHOP$^{-/-}$ mice via tail vein injection.[28] The expression of CHOP in bone marrow cells was quantified by reverse-transcription polymerase chain reaction 2 weeks after bone marrow transplantation (BMT). The perivascular cuff was placed 2 weeks after BMT; histological analysis was performed 3 weeks after cuff placement. Similarly, CHOP$^{+/+}$;apoE$^{-/-}$ and CHOP$^{-/-}$;apoE$^{-/-}$ recipient mice at 8 weeks of age underwent 10-Gy irradiation and then received 4×10^6 freshly prepared sterile bone marrow cells obtained from CHOP$^{+/+}$;apoE$^{-/-}$ and CHOP$^{-/-}$;apoE$^{-/-}$ recipient mice via tail vein injection. The mice were fed standard chow for 2 weeks after BMT and then a 1.25% high-cholesterol diet for the following 12 weeks.

Ex Vivo Treatment of Macrophages

Peritoneal macrophages were harvested from lavage of CHOP$^{+/+}$ and CHOP$^{-/-}$ mice 4 days after intraperitoneal injection of 4% thioglycollate. Macrophages were cultured in RPMI 1640 containing 10% FBS. Two hours later, nonadherent cells were flushed out and fresh medium was added. After 24 hours, the cells were incubated

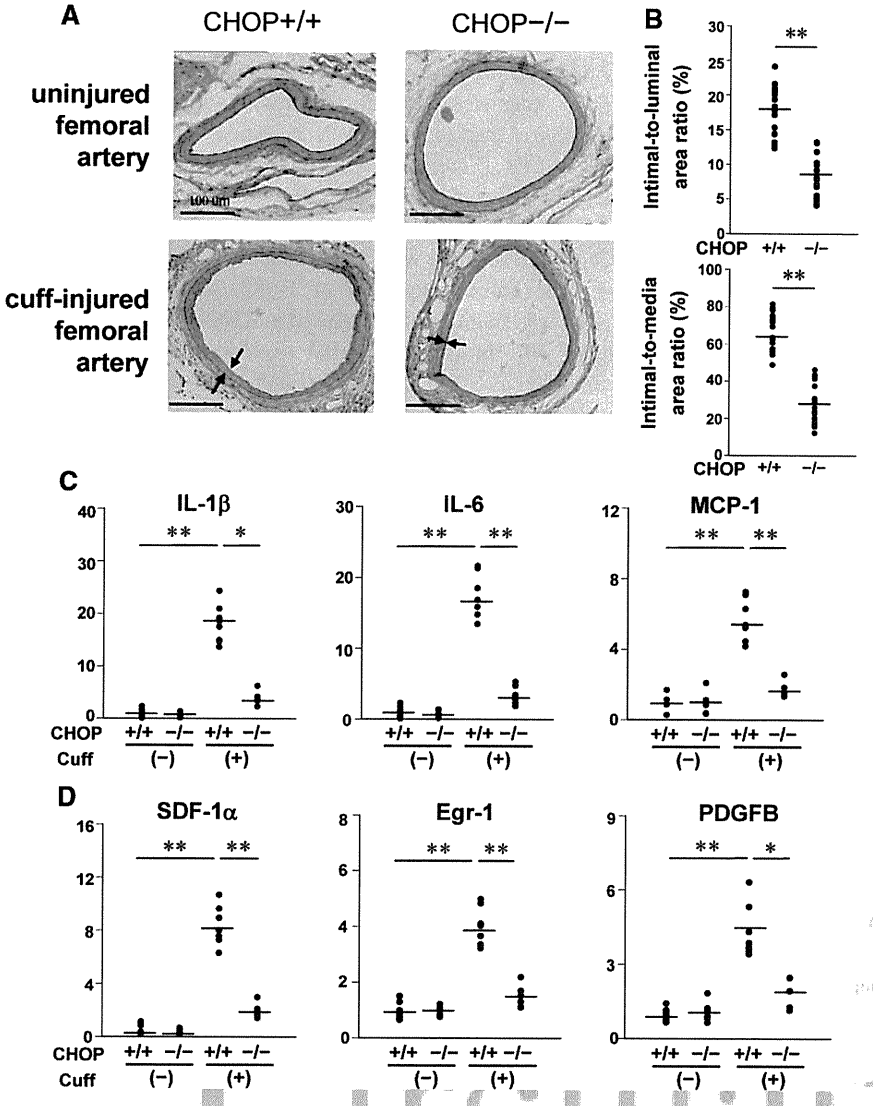

Figure 1. Roles of C/EBP homologous protein (CHOP) in arterial neointimal formation induced by cuff injury. **A**, Representative histological findings of uninjured (top) or cuff-injured (bottom) femoral arteries from CHOP$^{+/+}$ (left) and CHOP$^{-/-}$ (right) mice. Spaces between arrows indicate intimal areas. **B**, Intimal-to-luminal and intimal-to-medial area ratios of cuff-injured femoral arteries of CHOP$^{+/+}$ (n=19) and CHOP$^{-/-}$ (n=21) mice. **C** and **D**, Expression of inflammatory factors (interleukin [IL]-1β, IL-6, and monocyte chemoattractant protein-1 [MCP-1]) (**C**) and vascular smooth muscle cell (SMC) proliferation–related factors (stromal cell-derived factor-1α [SDF-1α], early growth response protein-1 [Egr1], and platelet-derived growth factor-b [PDGFB]) (**D**) in cuff-injured and uninjured arteries 7 days after cuff placement in CHOP$^{+/+}$ and CHOP$^{-/-}$ (n=7 per group) mice was quantified by reverse-transcription polymerase chain reaction adjusted with α-actin. Data are presented as mean±SE. *P<0.05, **P<0.01 by the unpaired t test or 1-way ANOVA.

with 0.25 μmol/L thapsigargin (Sigma-Aldrich Inc, St. Louis, MO) for 4 hours, 1 mmol/L peroxynitrite (Cayman Chemical Co) for 3 hours, or 100 μg/mL acetyl-LDL (Biomedical Technologies Inc, Stoughton, MA) plus the acyl-CoA:cholesterol acyltransferase inhibitor CI976 (Sigma-Aldrich Inc; 10 μmol/L) for 5 hours.

Cell Culture and siRNA Transfection

Mouse endothelial MSS31 cells, provided by Dr Yasufumi Sato (Tohoku University), and human aortic smooth muscle cells (SMCs; KURABO, Osaka, Japan) were cultured in α minimum essential medium containing 5% FBS and Humedia-SG2 (KURABO), respectively. Human and mouse CHOP small interfering RNAs (siRNAs) and control siRNAs were designed in conjunction with Thermo Fisher Scientific Inc (Yokohama, Japan). siRNAs and the transfection reagent DharmaFECT (Thermo Fisher scientific Inc, Yokohama, Japan) were added to the medium, followed by incubation for 24 hours at 37°C. siRNA-transfected human aortic SMCs and MSS31 were incubated with thapsigargin (0.75 μmol/L) and tunicamycin (2.5 μg/mL), respectively, for 10 hours.

Statistical Analysis

All statistical analyses were performed with the SPSS version 15.0 (SPSS Japan Inc, Tokyo, Japan). All data were tested for normality by the Kolmogorov-Smirnov test. When data were normally distributed, the statistical significance of differences was assessed with the unpaired t test and 1-way ANOVA, followed by Tukey post hoc analyses. When data were not normally distributed, the statistical significance of differences was judged on the basis of P values with the Mann–Whitney U test.

Results

C/EBP Homologous Protein Deficiency Suppresses Neointimal Formation Induced by Cuff Injury

The CHOP$^{+/+}$ and CHOP$^{-/-}$ mice were fed normal chow and comparatively analyzed at 11 weeks of age. As reported previously,[29] CHOP deletion did not significantly affect overall body weight, blood glucose, blood pressure, or plasma lipid parameters (Figure IA through ID in the online-only Data Supplement). Although plasma adiponectin levels were slightly higher in CHOP$^{-/-}$ mice, no significant differences were observed in serum MCP-1 or tumor necrosis factor-α levels between CHOP$^{+/+}$ and CHOP$^{-/-}$ mice (Figure IE in the online-only Data Supplement).

First, to assess the role of CHOP in vascular remodeling, we evaluated the effects of CHOP deficiency on neointimal formation induced by cuff injury. There were no apparent histological differences between uninjured femoral arteries in CHOP$^{+/+}$ and CHOP$^{-/-}$ mice (Figure 1A). In contrast, in

cuff-injured femoral arteries, $CHOP^{-/-}$ mice exhibited significant suppression of intimal hyperplasia (Figure 1A). The intimal hyperplasia was also quantified as intimal-to-luminal and intimal-to-medial area ratios, which were decreased by 56.4% and 56.0%, respectively, in $CHOP^{-/-}$ mice compared with $CHOP^{+/+}$ mice (Figure 1B).

Arterial wall intimal hyperplasia is reportedly attributable to heightened inflammatory reactions induced by interactions between recruited leukocytes and migrating SMCs.[30] Therefore, we next examined the local expression of genes related to vascular remodeling in cuff-injured femoral arteries 7 days after cuff placement. First, CHOP was markedly upregulated by cuff injury in $CHOP^{+/+}$ mice (Figure II in the online-only Data Supplement). In uninjured femoral arteries, there were no significant differences in the expression of inflammatory factors or vascular SMC proliferation–related factors between $CHOP^{+/+}$ and $CHOP^{-/-}$ mice (Figure 1C and 1D). In contrast, in cuff-injured femoral arteries, expression of inflammatory factors such as interleukin (IL)-1β, IL-6, and MCP-1 was significantly suppressed in $CHOP^{-/-}$ mice compared with $CHOP^{+/+}$ mice (Figure 1C). In addition, CHOP deficiency inhibited increased expression of vascular SMC proliferation–related factors such as stromal cell-derived factor-1α (also known as CXCL12), early growth response protein-1, and platelet-derived growth factor-B (Figure 1D). As a result, cuff injury–induced expression of α-smooth muscle actin was markedly suppressed in the arteries of $CHOP^{-/-}$ mice (Figure IIIA in the online-only Data Supplement). Immunostaining with antibodies against α-smooth muscle actin revealed that CHOP deficiency decreased α-smooth muscle actin staining in the neointima of cuff-injured arteries (Figure IIIB in the online-only Data Supplement). Furthermore, proliferating cell nuclear antigen–positive cells in the neointima were significantly decreased in $CHOP^{-/-}$ mice (Figure IIIC in the online-only Data Supplement). Taken together, these findings suggest that CHOP exacerbates cuff injury–induced inflammation and SMC proliferation, leading to vascular remodeling.

C/EBP Homologous Protein Deficiency Suppressed Hypercholesterolemia-Induced Atherosclerosis in $ApoE^{-/-}$ Mice

Next, to examine whether CHOP is involved in hypercholesterolemia-induced atherosclerosis, $CHOP^{-/-}$ mice were crossed with apoE-deficient mice, resulting in the generation of $CHOP^{-/-}$;$apoE^{-/-}$ double-knockout mice. The $CHOP^{+/+}$;$apoE^{-/-}$ and $CHOP^{-/-}$;$apoE^{-/-}$ mice were fed a 1.25% high-cholesterol chow starting at 8 weeks of age. In this hypercholesterolemia model, body weight, blood glucose, blood pressure, and lipid parameters were similar in $CHOP^{+/+}$;$apoE^{-/-}$ and $CHOP^{-/-}$;$apoE^{-/-}$ mice (Figure IV in the online-only Data Supplement). Interestingly, atherosclerosis development was significantly inhibited by CHOP deficiency. The atherosclerotic areas were decreased by 31% in the whole aortas of $CHOP^{-/-}$;$apoE^{-/-}$ compared with those of $CHOP^{+/+}$;$apoE^{-/-}$ mice at 32 weeks of age, as defined by Oil Red O staining (Figure 2A). Histological analyses of aortic root cross sections of $CHOP^{+/+}$;$apoE^{-/-}$ and $CHOP^{-/-}$;$apoE^{-/-}$ (n=5, each) mice revealed that CHOP deficiency modestly inhibited atherosclerosis development even at 20 weeks of age (Figure V in the online-only Data Supplement).

Aortic sections from $CHOP^{-/-}$;$apoE^{-/-}$ and $CHOP^{+/+}$;$apoE^{-/-}$ mice were immunostained with antibodies against the macrophage marker MOMA-2, α-smooth muscle actin, and oxidized LDL (Figure VI in the online-only Data Supplement). A CHOP deficiency apparently decreased depositions of macrophages, SMCs, and oxidized LDL in the plaques of $apoE^{-/-}$ mice. These findings were compatible with aortic gene expression. The aortic expression of F4/80, another macrophage marker, was significantly decreased in $CHOP^{-/-}$;$apoE^{-/-}$ mice (Figure 2B). In addition, aortic expression of inflammatory factors such as MCP-1 and IL-6 (Figure 2C); the ER chaperone Bip (Figure 2D); SMC proliferation–related genes such as transforming growth factor-β1, platelet-derived growth factor-B, and platelet-derived growth factor-Rβ (Figure 2E); and scavenger receptors such as mouse class A type I scavenger receptor and CD36 (Figure 2F) was significantly decreased in $CHOP^{-/-}$;$apoE^{-/-}$ mice. Decrements in protein expression of Bip and mouse class A type I scavenger receptor were confirmed by immunoblotting (Figure VII in the online-only Data Supplement). Furthermore, the plasma adiponectin level was increased whereas MCP-1 and tumor necrosis factor-α were significantly decreased in $CHOP^{-/-}$;$apoE^{-/-}$ mice (Figure 2G). Oxidative stress reportedly decreases plasma adiponectin.[31] In addition, CHOP deficiency markedly decreased plasma levels of oxidative stress markers such as malondialdehyde and 8-isoprostane (Figure 2H). Thus, CHOP appears to be involved in hypercholesterolemia-induced vascular inflammation and systemic oxidative stress, leading to atherosclerosis development.

C/EBP Homologous Protein Deficiency Suppressed Gene Expressions of Inflammation-Related Factors and Vascular Adhesion Molecules in Early-Stage Atherosclerosis

To examine the effects of CHOP deficiency on early-stage atherosclerosis, mRNA expression of inflammatory factors and vascular adhesion molecules was analyzed in the aortas of $CHOP^{-/-}$;$apoE^{-/-}$ and $CHOP^{+/+}$;$apoE^{-/-}$ mice at 14 weeks of age, when there were no apparent differences in Oil Red O–stained plaque areas between these 2 groups (Figure VIII in the online-only Data Supplement). Aortic expression of F4/80 and inflammatory factors such as MCP-1, IL-1β, and IL-6 was significantly decreased in $CHOP^{-/-}$;$apoE^{-/-}$ mice compared with $CHOP^{+/+}$;$apoE^{-/-}$ mice (Figure 3A), suggesting decreased aortic inflammation. In addition, expression of the vascular cell adhesion molecule-1 was decreased in $CHOP^{-/-}$;$apoE^{-/-}$ mice (Figure 3B). A CHOP deficiency also suppressed the aortic expression of GADD34 and ERO1α (Figure 3C), which are reportedly upregulated downstream from CHOP by ER stress. Furthermore, antioxidant enzymes such as manganese superoxide dismutase, glutathione-S-transferase, and catalase, which are upregulated in response to oxidative stress, were attenuated by CHOP deficiency (Figure 3D). These findings suggest that CHOP deficiency protects the arterial wall from both hypercholesterolemia-induced ER stress and oxidative stress. ERO1α downregulation may explain the decreased oxidative stress observed in $CHOP^{-/-}$;$apoE^{-/-}$ mice. Thus, CHOP is

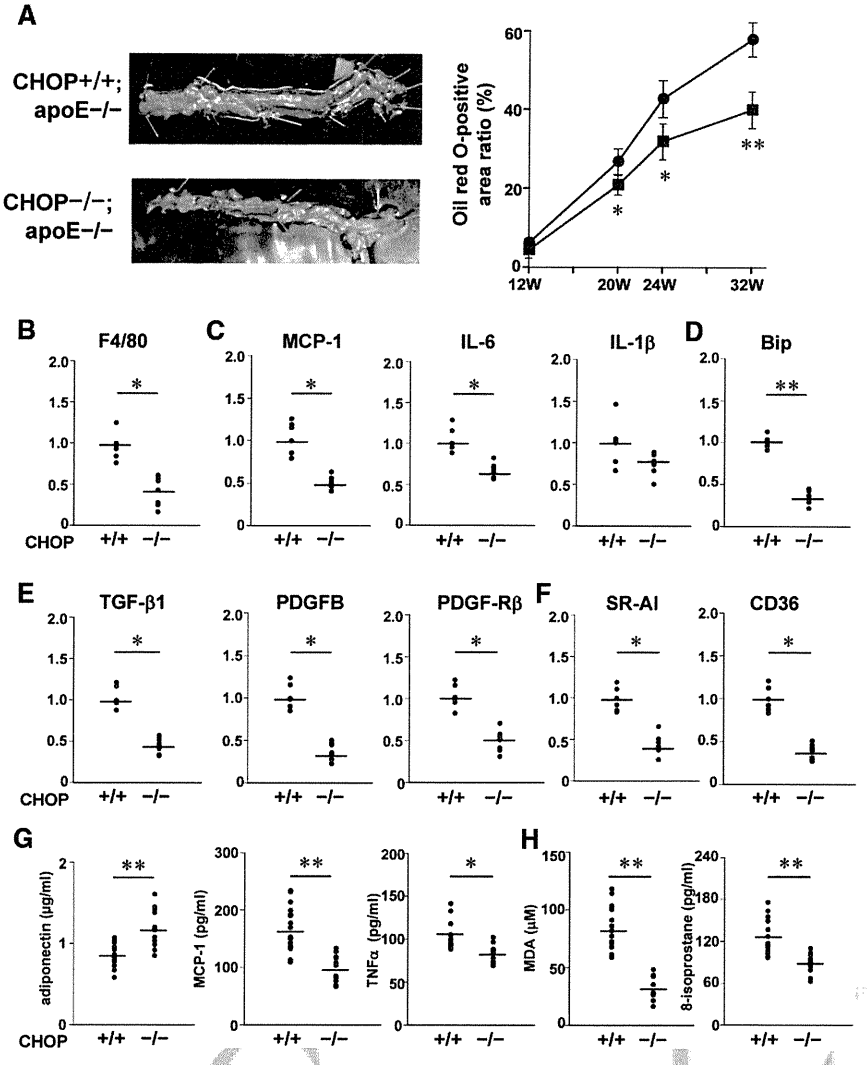

Figure 2. C/EBP homologous protein (CHOP) deficiency suppressed hypercholesterolemia-induced atherosclerosis in apoE$^{-/-}$ mice. The CHOP$^{+/+}$;apoE$^{-/-}$ and CHOP$^{-/-}$;apoE$^{-/-}$ mice were fed 1.25% high-cholesterol chow starting at 8 weeks of age. **A**, Atherosclerosis was evaluated as the Oil Red O–positive area, which was expressed as percentages of the total aortic areas in CHOP$^{+/+}$;apoE$^{-/-}$ (●, n=12 each) and CHOP$^{-/-}$;apoE$^{-/-}$ (■, n=9 each) mice from 12 to 32 weeks of age. Representative histological findings of whole aortas at 32 weeks of age are shown on the left. **B** through **F**, Aortic gene expression of the macrophage marker F4/80 (**B**); inflammatory factors such as monocyte chemoattractant protein-1 (MCP-1), interleukin (IL)-6 and IL-1β (**C**); an endoplasmic reticulum chaperone, Bip (**D**); smooth muscle cell proliferation–related genes such as transforming growth factor-β1 (TGF-β1), platelet-derived growth factor (PDGF)-B, and PDGF-Rβ (**E**); and scavenger receptors such as class A type I scavenger receptor (SR-AI) and CD36 (**F**) was analyzed in CHOP$^{+/+}$;apoE$^{-/-}$ (n=5) and CHOP$^{-/-}$;apoE$^{-/-}$ (n=7) mice at 24 weeks of age by reverse-transcription polymerase chain reaction. **G** through **H**, Plasma levels of adipokines (**G**) such as adiponectin, MCP-1, and tumor necrosis factor-α (TNF-α) and oxidized stress markers such as malondialdehyde (MDA) and 8-isoprostane (**H**) were measured in CHOP$^{+/+}$;apoE$^{-/-}$ (n=15) and CHOP$^{-/-}$;apoE$^{-/-}$ (n=16) mice at 24 weeks of age. Data are presented as mean±SE. $^{*}P<0.05$, $^{**}P<0.01$ by the unpaired *t* test, except for the atherosclerotic area at the age of 24 weeks (**A**) and F4/80 expression (**B**), which were analyzed with the Mann–Whitney *U* test.

likely to play important roles in promoting inflammation and adhesion molecule expression through oxidative stress and ER stress, thereby leading to atherosclerosis development.

C/EBP Homologous Protein, Especially in Vascular Cells, Is Involved in Cuff Injury–Induced Vascular Remodeling and Hypercholesterolemia-Induced Atherosclerosis

Thus, whole-body CHOP deficiency suppressed 2 types of arteriosclerosis, ie, cuff injury-induced neointimal formation and hypercholesterolemia-induced atherosclerosis. Both types of arteriosclerosis are well known to be caused by interactions between vascular cells such as endothelial cells and SMCs and hematopoietic cells such as macrophages. To determine which CHOP, that expressed in vascular cells or that expressed in hematopoietic cells, is important for these types of arteriosclerosis, we performed BMT experiments.

First, a series of BMT experiments, CHOP$^{+/+}$ to CHOP$^{+/+}$, CHOP$^{-/-}$ to CHOP$^{+/+}$, CHOP$^{+/+}$ to CHOP$^{-/-}$, and CHOP$^{-/-}$ to CHOP$^{-/-}$, was carried out in 6-week-old mice followed by external vascular cuff placement on the femoral arteries 2 weeks after BMT. At that time point, ie, 2 weeks after BMT, CHOP expression of BM cells in CHOP$^{-/-}$ to CHOP$^{+/+}$ BMT mice was markedly low (Figure IXA in the online-only Data Supplement), suggesting successful reconstitution of BM after transplantation. In addition, peripheral white blood cells decreased rapidly until day 3 after lethal irradiation and then recovered to pre-BMT levels within 13 days (Figure IXB in the online-only Data Supplement), indicating that BM cells had been mostly replaced with donor cells. In addition, in CHOP$^{+/+}$ to CHOP$^{+/+}$ BMT mice, arterial expression of both F4/80 and CD45 was dramatically increased, by 22- and 53-fold, respectively, during cuff injury, suggesting that almost all hematopoietic cells, including macrophages, in cuff-injured arteries had infiltrated the vascular wall after BMT and cuff placement (Figure X in the online-only Data Supplement). Under these conditions, neointimal formation was markedly suppressed in the CHOP$^{-/-}$ to CHOP$^{-/-}$ BMT mice compared with the CHOP$^{+/+}$ to CHOP$^{+/+}$ BMT mice. Both CHOP$^{-/-}$ to CHOP$^{+/+}$ and CHOP$^{+/+}$ to CHOP$^{-/-}$ mice exhibited intermediate degrees of neointimal formation, but recipient CHOP deficiency alone more strongly suppressed neointimal formation than donor deficiency alone (Figure 4). These findings suggest that CHOP expressed in hematopoietic and vascular cells may act in coordination to promote cuff injury–induced vascular

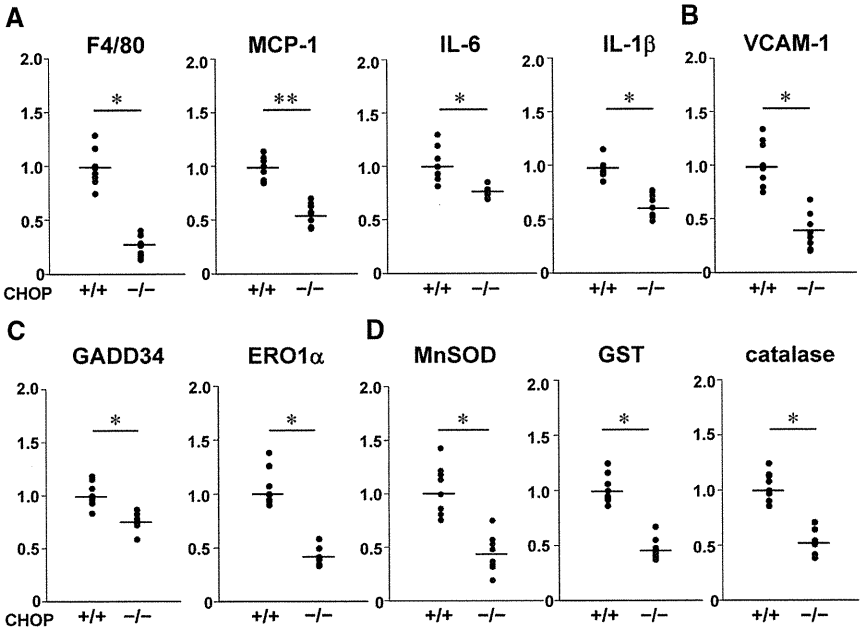

Figure 3. C/EBP homologous protein (CHOP) deficiency suppressed aortic expression of molecules related to inflammation and endoplasmic reticulum (ER) and oxidative stress in early-stage atherosclerosis in apoE$^{-/-}$ mice. Aortic gene expression of a macrophage marker and inflammatory factors (**A**), vascular cell adhesion molecule-1 (VCAM-1) (**B**), ER stress–related molecules (**C**), and antioxidant enzymes (**D**) was analyzed by reverse-transcription polymerase chain reaction in 14-week-old CHOP$^{+/+}$; apoE$^{-/-}$ and CHOP$^{-/-}$;apoE$^{-/-}$ mice fed 1.25% high-cholesterol chow (n=7 per group). Data are presented as mean±SE. MCP indicates monocyte chemoattractant protein; IL, interleukin; ERO1α, ER oxidase 1; MnSOD, manganese superoxide dismutase; and GST, glutathione-S-transferase. *P<0.05, **P<0.01 by the unpaired t test, except for MnSOD expression (**D**), which was analyzed with the Mann–Whitney U test.

remodeling, although vascular cell CHOP plays the more important role.

Next, BMT experiments were performed with 8-week-old CHOP$^{+/+}$;apoE$^{-/-}$ and CHOP$^{-/-}$;apoE$^{-/-}$ mice. Two weeks after BMT, high-cholesterol chow feeding was started and continued until 22 weeks of age. Both CHOP$^{-/-}$; apoE$^{-/-}$ to CHOP$^{+/+}$;apoE$^{-/-}$ and CHOP$^{+/+}$;apoE$^{-/-}$ to CHOP$^{-/-}$;apoE$^{-/-}$ mice apparently exhibited intermediate degrees of plaque formation. However, recipient CHOP deficiency significantly decreased atherosclerotic areas in apoE$^{-/-}$ mice, whereas the decreases in atherosclerotic areas with donor CHOP deficiency were not statistically significant. In addition, recipient CHOP deficiency more strongly decreased atherosclerotic areas than donor CHOP deficiency (Figure 5). These findings suggest that CHOP in recipient cells, including vascular cells, contributes to hypercholesterolemia-induced atherosclerosis.

Endoplasmic Reticulum Stress–Induced Biological Stress Responses That Were Suppressed by Decreased C/EBP Homologous Protein Expression in Macrophages and Vascular Cells

To determine the molecular mechanisms underlying the atherogenic actions of CHOP, we examined the effects of decreased CHOP expression on ER stress responses in macrophages and in SMC and endothelial cell lines in vitro. First, in peritoneal macrophages obtained from wild-type mice, treatment with thapsigargin, an ER stress inducer, markedly increased CHOP expression. In addition, inflammatory cytokines such as IL-6, MCP-1, and tumor necrosis factor-α were markedly upregulated in wild-type macrophages. These inflammatory responses to thapsigargin were significantly suppressed in macrophages obtained from CHOP$^{-/-}$ mice (Figure 6A). Furthermore, peroxynitrite[32] and free cholesterol[11] also increased the expression of both CHOP and inflammatory cytokines, but CHOP deficiency suppressed the inflammatory cytokine upregulation in macrophages (Figure XI in the online-only Data Supplement). Thus, CHOP upregulation appears to be involved in ER stress–induced inflammatory responses in macrophages.

Next, we examined alterations in gene expression with CHOP knockdown in a human aortic SMC line in response to thapsigargin treatment. In human aortic SMCs, thapsigargin upregulated CHOP and proliferation-related genes such as platelet-derived growth factor-B and stromal cell-derived factor-1α, as well as the inflammatory factor MCP-1 (Figure 6B). Knockdown of CHOP significantly suppressed the upregulation of proliferation- and inflammation-related factors. In addition, in a murine endothelial cell line, MSS31, tunicamycin, another ER stress inducer, increased the expression of ER stress–related proteins such as CHOP, GADD34, and ERO1α, but these increments were significantly inhibited by CHOP knockdown (Figure 6C), suggesting a role of CHOP in accelerating UPRs. Furthermore, CHOP knockdown blocked tunicamycin-induced upregulation of vascular cell adhesion molecule-1 in endothelial cells. These in vitro experiments revealed that ER stress promotes the proliferation of SMCs and adhesion molecule upregulation in endothelial cells. Thus, CHOP augments these stress responses in vascular cells. Collectively, CHOP, in both macrophages and vascular cells, is likely to exert atherogenic effects via heightened biological stress responses, including inflammation-, adhesion-, or SMC proliferation–related protein upregulation.

Discussion

The first important result obtained in this study is that CHOP deficiency inhibited cuff injury–induced neointimal formation. Neointimal formation, which is an important feature of restenosis after angioplasty of human coronary arteries,[33] critically involves the proliferation and migration of vascular SMCs. In the cuff injury model, adventitial inflammation is considered to be a major cause of medial SMC migration to the subendothelial space.[30] In the present study, CHOP deficiency suppressed aortic expression of inflammatory

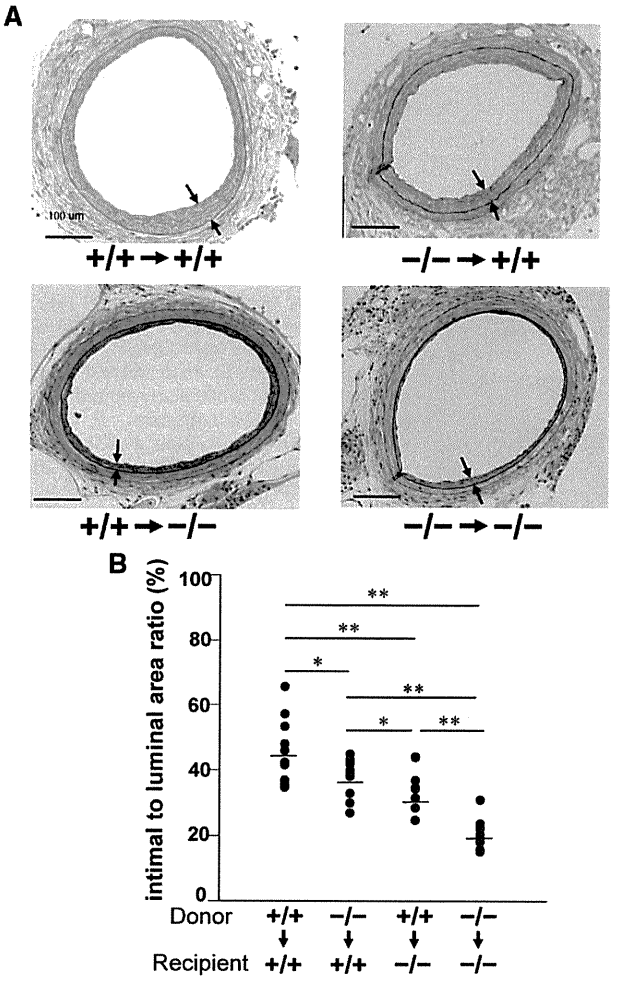

Figure 4. Importance of C/EBP homologous protein (CHOP) in vascular cells in cuff injury–induced vascular remodeling. A series of bone marrow transplantation (BMT) experiments, $CHOP^{+/+}$ to $CHOP^{+/+}$, $CHOP^{-/-}$ to $CHOP^{+/+}$, $CHOP^{+/+}$ to $CHOP^{-/-}$, and $CHOP^{-/-}$ to $CHOP^{-/-}$, was carried out in 6-week-old mice. Bone marrow cells from $CHOP^{+/+}$ and $CHOP^{-/-}$ mice were transplanted into lethally irradiated $CHOP^{+/+}$ and $CHOP^{-/-}$ mice. Perivascular cuffs were placed on the femoral arteries 2 weeks after BMT, followed by analysis of neointimal formation 3 weeks later. **A**, Representative histological findings of cuff-injured femoral arteries from the indicated mice. **B**, Intimal-to-luminal area ratios of cuff-injured femoral arteries of mice subjected to BMT ($CHOP^{+/+}$ to $CHOP^{+/+}$, n=10; $CHOP^{-/-}$ to $CHOP^{+/+}$, n=10; $CHOP^{+/+}$ to $CHOP^{-/-}$, n=10; $CHOP^{-/-}$ to $CHOP^{-/-}$, n=9). Data are presented as mean±SE. $^{*}P<0.05$, $^{**}P<0.01$ by 1-way ANOVA.

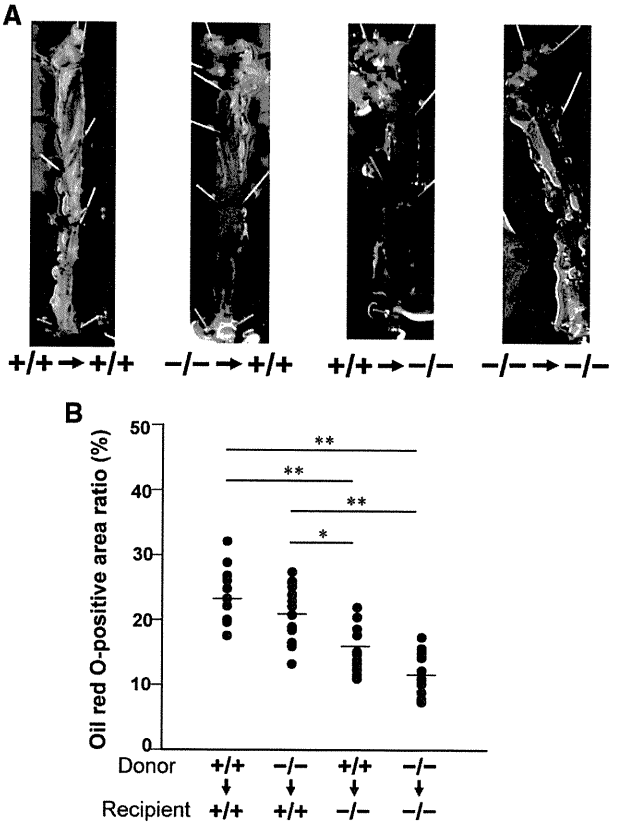

Figure 5. Importance of C/EBP homologous protein (CHOP) in vascular cells in hypercholesterolemia-induced atherosclerosis. A series of bone marrow transplantation (BMT) experiments, $CHOP^{+/+}$;$apoE^{-/-}$ to $CHOP^{+/+}$;$apoE^{-/-}$, $CHOP^{-/-}$;$apoE^{-/-}$ to $CHOP^{+/+}$;$apoE^{-/-}$, $CHOP^{+/+}$;$apoE^{-/-}$ to $CHOP^{-/-}$;$apoE^{-/-}$, and $CHOP^{-/-}$;$apoE^{-/-}$ to $CHOP^{-/-}$;$apoE^{-/-}$, was carried out in 8-week-old mice. Two weeks after BMT, 1.25% high-cholesterol chow feeding was started. Oil Red O–stained areas of the aortas of these BMT mice were measured at 22 weeks of age ($CHOP^{+/+}$;$apoE^{-/-}$ to $CHOP^{+/+}$;$apoE^{-/-}$, n=10; $CHOP^{-/-}$;$apoE^{-/-}$ to $CHOP^{+/+}$;$apoE^{-/-}$, n=14; $CHOP^{+/+}$;$apoE^{-/-}$ to $CHOP^{-/-}$;$apoE^{-/-}$, n=13; $CHOP^{-/-}$;$apoE^{-/-}$ to $CHOP^{-/-}$;$apoE^{-/-}$, n=10) (**B**). Representative histological findings of the whole aorta and plaque are shown in **A**. Data are presented as mean±SE. $^{*}P<0.05$, $^{**}P<0.01$ by 1-way ANOVA.

factors and growth factors that induce vascular SMC proliferation. In addition, BMT experiments revealed a small but significant effect of CHOP donor deficiency. Because almost all hematopoietic cells, which were detected in the aorta 3 weeks after cuff placement, had infiltrated the aorta after cuff placement following bone marrow replacement, the small but significant effect of CHOP donor deficiency actually reflects the positive contribution of CHOP expressed in hematopoietic cells. On the other hand, recipient CHOP deficiency more strongly suppressed cuff injury–induced neointimal formation than donor CHOP deficiency, indicating the importance of recipient CHOP in vascular remodeling. We cannot rule out the possibility that CHOP expressed in recipient cells other than vascular cells is involved in vascular remodeling. However, taken together with the findings that CHOP deficiency suppressed vascular expressions of inflammatory factors and stress-related proteins and that CHOP in endothelial cells and vascular SMCs contributes to upregulation of these factors in vitro, CHOP in vascular cells is likely to play important roles. Thus, CHOP expressed in both hematopoietic cells and vascular cells, especially that expressed in vascular cells, contributes to vascular remodeling. Our in vitro results further support the notion that CHOP expressed in hematopoietic and vascular cells acts in a coordinated fashion to exacerbate arterial inflammation, which leads to vascular remodeling.

Another important aspect of the present study is that activation of CHOP was shown to play an important role in hypercholesterolemia-induced progression of atherosclerosis; CHOP is well known to be a strong mediator of apoptosis induction in cells exposed to substantial ER stress.[34] Aortic expression of CHOP is enhanced as atherosclerosis pro-

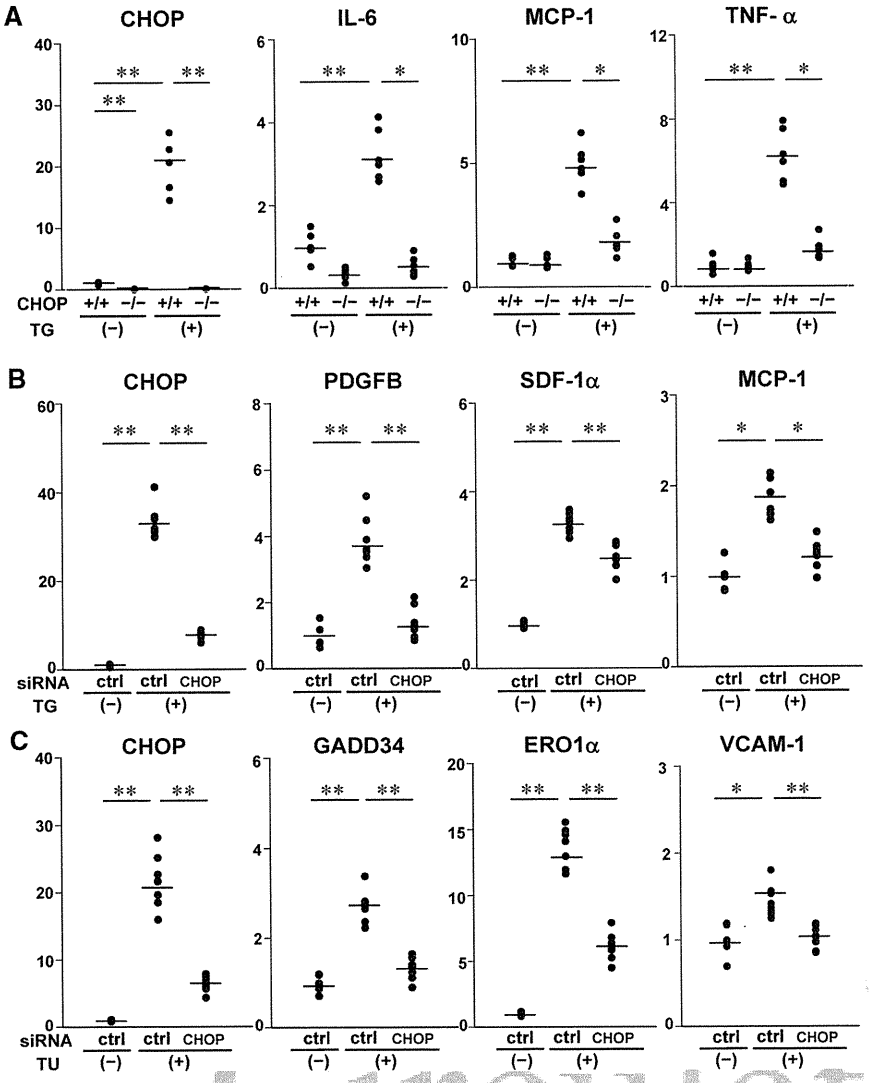

Figure 6. C/EBP homologous protein (CHOP) deficiency or knockdown suppressed inflammatory and endoplasmic reticulum (ER) stress responses of macrophages and vascular cells. **A**, mRNA expression of CHOP and inflammatory cytokines in peritoneal macrophages from $CHOP^{+/+}$ (n=5) and $CHOP^{-/-}$ (n=5) mice with thapsigargin (TG) treatment was evaluated by reverse-transcription polymerase chain reaction (RT-PCR). Peritoneal macrophages from $CHOP^{+/+}$ (n=4) and $CHOP^{-/-}$ (n=6) mice without thapsigargin treatment were also subjected to analyses of mRNA expression. **B**, Human aortic smooth muscle cells (HASMCs) were transfected with siRNA against the human CHOP gene (n=7) or scramble control (ctrl; n=7), followed by thapsigargin treatment. The mRNA expression of CHOP, proliferation-related genes, and an inflammatory factor was evaluated by RT-PCR procedures. The HASMCs transfected with scramble siRNA without thapsigargin treatment (n=4) were also subjected to analyses of mRNA expression. **C**, MSS31 cells were transfected with siRNA against the murine CHOP gene (n=7) or scramble control (n=7), followed by tunicamycin (TU) treatment. The mRNA expression of CHOP, GADD34, ER oxidase 1 (ERO1α) and vascular cell adhesion molecule-1 (VCAM-1) was evaluated by RT-PCR procedures. MSS31 cells transfected with scramble siRNA without tunicamycin treatment (n=4) were also subjected to analyses of mRNA expression. Data are presented as mean±SE. $^{*}P<0.05$, $^{**}P<0.01$ by 1-way ANOVA.

gresses.[10] In atherosclerotic lesions, apoptotic cells, which are derived mainly from macrophages but to a lesser extent endothelial and SMCs, are increased.[35] Apoptotic macrophages release proteases and inflammatory factors and induce lipid core formation. Free cholesterol accumulation in the ER membranes of macrophages reportedly induces the UPR, leading to CHOP-mediated apoptotic cell death.[11] Thorp and colleagues[17] reported that CHOP deficiency suppressed atherosclerotic progression in $apoE^{-/-}$ mice, which is consistent with our results. They concluded that the mechanism underlying atherosclerotic inhibition with CHOP deficiency involves decreased atherosclerotic plaque necrosis and lesional apoptosis of macrophages. The CHOP-mediated apoptosis in macrophages also reportedly contributes to the instability of atherosclerotic plaques,[36] suggesting the importance of macrophage CHOP. In addition to the roles of macrophage CHOP, our study shows vascular CHOP to have a significant role. First, BMT experiments revealed that CHOP deficiency in recipient mice more strongly suppressed atherosclerosis development than that in donor mice. We cannot rule out the possibility that residual macrophages that had infiltrated the aorta before BMT weakened the suppressive effects of donor CHOP deficiency. Even if this were the case, however, the significant effects of recipient CHOP deficiency indicate that CHOP expressed in vascular cells plays an important role in atherosclerosis development. In addition, global CHOP deficiency decreased aortic macrophage deposition per se in the early stage, eg, at 14 weeks of age, leading to suppression of atherosclerosis development at 24 weeks of age. Therefore, decreased macrophage infiltration in the early stage is likely to be an important mechanism by which CHOP deficiency suppresses atherosclerosis development. Endothelial adhesion molecule expression was decreased by CHOP deficiency, and in vitro experiments revealed that CHOP knockdown in endothelial cells inhibited upregulation of the endothelial adhesion molecule. Together, these findings suggest that suppression of endothelial adhesion molecule expression by CHOP deficiency is involved in the infiltration of macrophages into the vascular wall. Therefore, suppressed macrophage-endothelium interaction resulting from CHOP deficiency in both cells is likely to contribute to inhibition of atherosclerosis development. In vitro experiments also revealed that CHOP knockdown in SMCs suppressed upregulation of inflammatory factors. Supporting this notion, CHOP

deficiency reduced aortic expression and plasma concentrations of inflammatory factors and oxidative stress markers. Thus, in addition to the reported mechanism involving macrophage apoptosis,[17] vascular CHOP in endothelial cells and SMCs plays important roles in atherosclerosis development via augmentation of macrophage recruitment and inflammatory and stress responses.

Interestingly, CHOP deficiency suppressed aortic expressions of Bip and GADD34 in apoE$^{-/-}$ mice, suggesting that CHOP also plays a role in accelerating UPRs other than those involved in the induction of apoptosis. This finding is consistent with a previous report indicating that, in CHOP$^{-/-}$ cells, GADD34 protein is downregulated in association with sustained elevation of eukaryotic initiation factor-2 α phosphorylation, followed by translation repression, resulting in reduced ER stress.[18] In addition, several reports have indicated that the UPR is closely related to inflammatory responses.[37] Inositol-requiring enzyme-1α activates the c-jun N-terminal kinase pathway, increasing the levels of tumor necrosis factor-α, IL-6, and MCP-1 through activation of the activator protein-1 transcription factor complex.[38] The nuclear factor-κB pathway can also be activated by PKR-like ER kinase signaling in both endothelial cells and macrophages.[11,14,39] Furthermore, CHOP directly induces expression of ERO1α, which is required for disulphide formation in protein folding and contributes to elevation of reactive oxygen species in ER-stressed cells.[40] Induction of ERO1α by CHOP might be involved in CHOP-mediated accumulation of reactive oxygen species.[41] Consistent with these previous studies, here, CHOP deficiency suppressed ERO1α expression in the aortas of apoE$^{-/-}$ mice. In addition, aortic expression of antioxidant enzymes was downregulated in CHOP$^{-/-}$;apoE$^{-/-}$ mice, suggesting a decrement in hypercholesterolemia-induced oxidative stress. Consistent with this notion, oxidative markers such as malondialdehyde and 8-isoprostane and adiponectin levels in apoE$^{-/-}$ mice were markedly decreased and increased, respectively, by CHOP deficiency. Thus, in addition to the well-known "canonical" signaling that triggers apoptosis induction, CHOP may play important roles in augmenting potentially pathological biological responses. This "noncanonical" role of CHOP may contribute to hypercholesterolemia-induced exacerbation of oxidative stress not only in the aorta but also systemically, leading to atherosclerosis progression.

Conclusions

This study provides strong evidence of the impact of CHOP, especially that expressed in vascular cells, on arteriosclerosis formation. The underlying mechanisms involve augmentation of unfavorable, ie, pathological, stress responses. This noncanonical role of CHOP is important in vascular remodeling and atherosclerosis. Therefore, blockade of the CHOP signaling pathway is a promising therapeutic strategy for atherosclerosis induced by hypercholesterolemia and restenosis after angioplasty.

Acknowledgments

We thank I. Sato, J. Fushimi, K. Kawamura, M. Aizawa, M. Hoshi, and T. Takasugi for technical support. We also appreciate T. Morita and J. Tatebe for useful guidance on the cuff injury technique.

Sources of Funding

This work was supported by Grants-in-Aid for Scientific Research (B2, 15390282) to Dr Katagiri and (21591122) Dr Ishigaki, by JSPS Fellows (20-08126) to Dr Gao, and by the Global COE Program to Drs Oka, Katagiri, and Gao from the Ministry of Education, Science, Sports and Culture of Japan of the Ministry of Health, Labor and Welfare of Japan.

Disclosures

None.

References

1. Ross R. The pathogenesis of atherosclerosis: a perspective for the 1990s. *Nature*. 1993;362:801–809.
2. Katagiri H, Yamada T, Oka Y. Adiposity and cardiovascular disorders: disturbance of the regulatory system consisting of humoral and neuronal signals. *Circ Res*. 2007;101:27–39.
3. Steinberg D. Atherogenesis in perspective: hypercholesterolemia and inflammation as partners in crime. *Nat Med*. 2002;8:1211–1217.
4. Ishigaki Y, Katagiri H, Gao J, Yamada T, Imai J, Uno K, Hasegawa Y, Kaneko K, Ogihara T, Ishihara H, Sato Y, Takikawa K, Nishimichi N, Matsuda H, Sawamura T, Oka Y. Impact of plasma oxidized low-density lipoprotein removal on atherosclerosis. *Circulation*. 2008;118:75–83.
5. Ishigaki Y, Oka Y, Katagiri H. Circulating oxidized LDL: a biomarker and a pathogenic factor. *Curr Opin Lipidol*. 2009;20:363–369.
6. Ron D, Walter P. Signal integration in the endoplasmic reticulum unfolded protein response. *Nat Rev Mol Cell Biol*. 2007;8:519–529.
7. Niwa M, Sidrauski C, Kaufman RJ, Walter P. A role for presenilin-1 in nuclear accumulation of Ire1 fragments and induction of the mammalian unfolded protein response. *Cell*. 1999;99:691–702.
8. Bi M, Naczki C, Koritzinsky M, Fels D, Blais J, Hu N, Harding H, Novoa I, Varia M, Raleigh J, Scheuner D, Kaufman RJ, Bell J, Ron D, Wouters BG, Koumenis C. ER stress-regulated translation increases tolerance to extreme hypoxia and promotes tumor growth. *EMBO J*. 2005;24:3470–3481.
9. Ishihara H, Takeda S, Tamura A, Takahashi R, Yamaguchi S, Takei D, Yamada T, Inoue H, Soga H, Katagiri H, Tanizawa Y, Oka Y. Disruption of the WFS1 gene in mice causes progressive beta-cell loss and impaired stimulus-secretion coupling in insulin secretion. *Hum Mol Genet*. 2004;13:1159–1170.
10. Zhou J, Lhotak S, Hilditch BA, Austin RC. Activation of the unfolded protein response occurs at all stages of atherosclerotic lesion development in apolipoprotein E-deficient mice. *Circulation*. 2005;111:1814–1821.
11. Feng B, Yao PM, Li Y, Devlin CM, Zhang D, Harding HP, Sweeney M, Rong JX, Kuriakose G, Fisher EA, Marks AR, Ron D, Tabas I. The endoplasmic reticulum is the site of cholesterol-induced cytotoxicity in macrophages. *Nat Cell Biol*. 2003;5:781–792.
12. Sanson M, Auge N, Vindis C, Muller C, Bando Y, Thiers JC, Marachet MA, Zarkovic K, Sawa Y, Salvayre R, Negre-Salvayre A. Oxidized low-density lipoproteins trigger endoplasmic reticulum stress in vascular cells: prevention by oxygen-regulated protein 150 expression. *Circ Res*. 2009;104:328–336.
13. Zhou J, Werstuck GH, Lhotak S, de Koning AB, Sood SK, Hossain GS, Moller J, Ritskes-Hoitinga M, Falk E, Dayal S, Lentz SR, Austin RC. Association of multiple cellular stress pathways with accelerated atherosclerosis in hyperhomocysteinemic apolipoprotein E-deficient mice. *Circulation*. 2004;110:207–213.
14. Gargalovic PS, Gharavi NM, Clark MJ, Pagnon J, Yang WP, He A, Truong A, Baruch-Oren T, Berliner JA, Kirchgessner TG, Lusis AJ. The unfolded protein response is an important regulator of inflammatory genes in endothelial cells. *Arterioscler Thromb Vasc Biol*. 2006;26:2490–2496.
15. Myoishi M, Hao H, Minamino T, Watanabe K, Nishihira K, Hatakeyama K, Asada Y, Okada K, Ishibashi-Ueda H, Gabbiani G, Bochaton-Piallat ML, Mochizuki N, Kitakaze M. Increased endoplasmic reticulum stress in atherosclerotic plaques associated with acute coronary syndrome. *Circulation*. 2007;116:1226–1233.
16. Oyadomari S, Mori M. Roles of CHOP/GADD153 in endoplasmic reticulum stress. *Cell Death Differ*. 2004;11:381–389.
17. Thorp E, Li G, Seimon TA, Kuriakose G, Ron D, Tabas I. Reduced apoptosis and plaque necrosis in advanced atherosclerotic lesions of Apoe−/− and Ldlr−/− mice lacking CHOP. *Cell Metab*. 2009;9:474–481.

18. Marciniak SJ, Yun CY, Oyadomari S, Novoa I, Zhang Y, Jungreis R, Nagata K, Harding HP, Ron D. CHOP induces death by promoting protein synthesis and oxidation in the stressed endoplasmic reticulum. *Genes Dev.* 2004;18:3066–3077.
19. Song B, Scheuner D, Ron D, Pennathur S, Kaufman RJ. Chop deletion reduces oxidative stress, improves beta cell function, and promotes cell survival in multiple mouse models of diabetes. *J Clin Invest.* 2008;118: 3378–3389.
20. Li G, Mongillo M, Chin KT, Harding H, Ron D, Marks AR, Tabas I. Role of ERO1-alpha-mediated stimulation of inositol 1,4,5-triphosphate receptor activity in endoplasmic reticulum stress-induced apoptosis. *J Cell Biol.* 2009;186:783–792.
21. Oyadomari S, Takeda K, Takiguchi M, Gotoh T, Matsumoto M, Wada I, Akira S, Araki E, Mori M. Nitric oxide-induced apoptosis in pancreatic beta cells is mediated by the endoplasmic reticulum stress pathway. *Proc Natl Acad Sci U S A.* 2001;98:10845–10850.
22. Gao J, Katagiri H, Ishigaki Y, Yamada T, Ogihara T, Imai J, Uno K, Hasegawa Y, Kanzaki M, Yamamoto TT, Ishibashi S, Oka Y. Involvement of apolipoprotein E in excess fat accumulation and insulin resistance. *Diabetes.* 2007;56:24–33.
23. Zhang SH, Reddick RL, Burkey B, Maeda N. Diet-induced atherosclerosis in mice heterozygous and homozygous for apolipoprotein E gene disruption. *J Clin Invest.* 1994;94:937–945.
24. Yamada T, Katagiri H, Ishigaki Y, Ogihara T, Imai J, Uno K, Hasegawa Y, Gao J, Ishihara H, Niijima A, Mano H, Aburatani H, Asano T, Oka Y. Signals from intra-abdominal fat modulate insulin and leptin sensitivity through different mechanisms: neuronal involvement in food-intake regulation. *Cell Metab.* 2006;3:223–229.
25. Moroi M, Zhang L, Yasuda T, Virmani R, Gold HK, Fishman MC, Huang PL. Interaction of genetic deficiency of endothelial nitric oxide, gender, and pregnancy in vascular response to injury in mice. *J Clin Invest.* 1998;101:1225–1232.
26. Ishigaki Y, Katagiri H, Yamada T, Ogihara T, Imai J, Uno K, Hasegawa Y, Gao J, Ishihara H, Shimosegawa T, Sakoda H, Asano T, Oka Y. Dissipating excess energy stored in the liver is a potential treatment strategy for diabetes associated with obesity. *Diabetes.* 2005;54:322–332.
27. Imai J, Katagiri H, Yamada T, Ishigaki Y, Suzuki T, Kudo H, Uno K, Hasegawa Y, Gao J, Kaneko K, Ishihara H, Niijima A, Nakazato M, Asano T, Minokoshi Y, Oka Y. Regulation of pancreatic beta cell mass by neuronal signals from the liver. *Science.* 2008;322:1250–1254.
28. Hasegawa Y, Ogihara T, Yamada T, Ishigaki Y, Imai J, Uno K, Gao J, Kaneko K, Ishihara H, Sasano H, Nakauchi H, Oka Y, Katagiri H. Bone marrow (BM) transplantation promotes beta-cell regeneration after acute injury through BM cell mobilization. *Endocrinology.* 2007;148: 2006–2015.
29. Oyadomari S, Koizumi A, Takeda K, Gotoh T, Akira S, Araki E, Mori M. Targeted disruption of the Chop gene delays endoplasmic reticulum stress-mediated diabetes. *J Clin Invest.* 2002;109:525–532.
30. Egashira K, Zhao Q, Kataoka C, Ohtani K, Usui M, Charo IF, Nishida K, Inoue S, Katoh M, Ichiki T, Takeshita A. Importance of monocyte chemoattractant protein-1 pathway in neointimal hyperplasia after periarterial injury in mice and monkeys. *Circ Res.* 2002;90:1167–1172.
31. Furukawa S, Fujita T, Shimabukuro M, Iwaki M, Yamada Y, Nakajima Y, Nakayama O, Makishima M, Matsuda M, Shimomura I. Increased oxidative stress in obesity and its impact on metabolic syndrome. *J Clin Invest.* 2004;114:1752–1761.
32. Dickhout JG, Hossain GS, Pozza LM, Zhou J, Lhotak S, Austin RC. Peroxynitrite causes endoplasmic reticulum stress and apoptosis in human vascular endothelium: implications in atherogenesis. *Arterioscler Thromb Vasc Biol.* 2005;25:2623–2629.
33. Libby P, Ganz P. Restenosis revisited–new targets, new therapies. *N Engl J Med.* 1997;337:418–419.
34. Ron D, Habener JF. CHOP, a novel developmentally regulated nuclear protein that dimerizes with transcription factors C/EBP and LAP and functions as a dominant-negative inhibitor of gene transcription. *Genes Dev.* 1992;6:439–453.
35. Hegyi L, Skepper JN, Cary NR, Mitchinson MJ. Foam cell apoptosis and the development of the lipid core of human atherosclerosis. *J Pathol.* 1996;180:423–429.
36. Tsukano H, Gotoh T, Endo M, Miyata K, Tazume H, Kadomatsu T, Yano M, Iwawaki T, Kohno K, Araki K, Mizuta H, Oike Y. The endoplasmic reticulum stress-C/EBP homologous protein pathway-mediated apoptosis in macrophages contributes to the instability of atherosclerotic plaques. *Arterioscler Thromb Vasc Biol.* 30:1925–1932.
37. Gregor MF, Hotamisligil GS. Thematic review series: adipocyte biology: adipocyte stress: the endoplasmic reticulum and metabolic disease. *J Lipid Res.* 2007;48:1905–1914.
38. Karin M, Gallagher E. From JNK to pay dirt: jun kinases, their biochemistry, physiology and clinical importance. *IUBMB Life.* 2005;57: 283–295.
39. Li Y, Schwabe RF, DeVries-Seimon T, Yao PM, Gerbod-Giannone MC, Tall AR, Davis RJ, Flavell R, Brenner DA, Tabas I. Free cholesterol-loaded macrophages are an abundant source of tumor necrosis factor-alpha and interleukin-6: model of NF-kappaB- and map kinase-dependent inflammation in advanced atherosclerosis. *J Biol Chem.* 2005; 280:21763–21772.
40. Harding HP, Zhang Y, Zeng H, Novoa I, Lu PD, Calfon M, Sadri N, Yun C, Popko B, Paules R, Stojdl DF, Bell JC, Hettmann T, Leiden JM, Ron D. An integrated stress response regulates amino acid metabolism and resistance to oxidative stress. *Mol Cell.* 2003;11:619–633.
41. McCullough KD, Martindale JL, Klotz LO, Aw TY, Holbrook NJ. Gadd153 sensitizes cells to endoplasmic reticulum stress by down-regulating Bcl2 and perturbing the cellular redox state. *Mol Cell Biol.* 2001;21:1249–1259.

CLINICAL PERSPECTIVE

Complex interactions among numerous biological pathways are implicated in the pathogenesis of arteriosclerosis such as atherosclerosis and vascular remodeling. In particular, responses to inflammation and oxidative stress have been considered to play central roles in arteriosclerosis development. In addition, recent studies revealed endoplasmic reticulum stress to be associated with atherosclerosis involving free cholesterol–induced macrophage apoptosis. However, details of the molecular mechanisms of interactions among classic atherogenic actions and endoplasmic reticulum stress responses remained to be elucidated. This study focused on the transcription factor C/EBP homologous protein (CHOP), which is well known to be induced by endoplasmic reticulum stress, mediating apoptotic cell death. Here, using CHOP-deficient mice, we show that CHOP plays important roles in accelerating 2 types of arteriosclerosis: cuff injury–induced neointimal formation and hypercholesterolemia-induced atherosclerosis. Augmented inflammatory and oxidative stress responses mediated by CHOP are important underlying mechanisms. Furthermore, CHOP, especially that expressed in hematopoietic and vascular cells, is involved in inflammatory interactions among macrophages, endothelial cells, and vascular smooth muscle cells, acting in a coordinated fashion to promote arteriosclerosis development. Thus, these observations of this noncanonical role of CHOP may lead to a better understanding of the molecular pathogenesis of vascular remodeling and atherosclerosis. Furthermore, given that neointimal formation is an important feature of postangioplasty restenosis of human coronary arteries, this study provides potential strategies for the prevention of cardiovascular diseases and the advancement of coronary intervention therapies.